Available online at www.sciencedirect.com
ScienceDirect
Bioorganic & Medicinal Chemistry 15 (2007) 7066–7086
Bioorganic & Medicinal Chemistry

Design and synthesis of manganese porphyrins with tailored lipophilicity: Investigation of redox properties and superoxide dismutase activity

Dorothée Lahaye,[a] Kannan Muthukumaran,[a] Chen-Hsiung Hung,[a] Dorota Gryko,[a] Júlio S. Rebouças,[b] Ivan Spasojević,[c] Ines Batinić-Haberle[b,*] and Jonathan S. Lindsey[a,*]

[a]*Department of Chemistry, North Carolina State University, Raleigh, NC 27695, USA*
[b]*Department of Radiation Oncology, Duke University Medical School, Durham, NC 27710, USA*
[c]*Department of Medicine, Duke University Medical School, Durham, NC 27710, USA*

Received 30 May 2007; revised 15 July 2007; accepted 17 July 2007
Available online 19 August 2007

Abstract—Thirteen new manganese porphyrins and two porphodimethenes bearing one to three different substituents at the *meso* positions in a variety of architectures have been synthesized. The substituents employed generally are (i) electron-withdrawing to tune the reduction potential to the desirable range (near +0.3 V vs NHE), and/or (ii) lipophilic to target the interior of lipid bilayer membranes and/or the blood–brain barrier. The influence of the substituents on the Mn^{III}/Mn^{II} reduction potentials has been characterized, and the superoxide dismutase activity of the compounds has been examined.

1. Introduction

Superoxide ($O_2^{\cdot-}$) is generated during the course of normal cellular metabolism but has highly adverse effects if not deactivated. The major sources of superoxide in vivo under physiological and pathological conditions stem from mitochondrial respiration and a variety of oxidases/oxygenases, particularly NADPH oxidase, xanthine oxidase, and the cytochrome P450 family.[1–4] Superoxide dismutase (SOD) deficiencies are associated with numerous human pathologies including pulmonary, cardiovascular, and degenerative diseases (stroke, Parkinson's, Huntington's, ALS, etc.).[4,5] Superoxide reacts with nitric oxide at diffusion-controlled rates, forming peroxynitrite ($ONOO^-$, ONOOH), a highly oxidizing species, which further decomposes to yield the hydroxyl radical ($^{\cdot}OH$) and the nitrogen dioxide radical ($^{\cdot}NO_2$). Peroxynitrite can also form an adduct with CO_2, giving rise to the carbonate radical anion ($CO_3^{\cdot-}$).[6] Thus, a therapeutic agent that could eliminate not only $O_2^{\cdot-}$, but also other oxidants ($ONOO^-$, $^{\cdot}NO_2$, and $CO_3^{\cdot-}$) would be advantageous.

The overall reaction of SOD enzymes ($O_2^{\cdot-} + O_2^{\cdot-} + 2H^+ \rightarrow O_2 + H_2O_2$) involves two half-reactions (Scheme 1).[2] The potential for the oxidation of $O_2^{\cdot-}$ is −0.160 V, while that for the reduction of $O_2^{\cdot-}$ is +0.890 V versus NHE in an aqueous medium.[7] The one-electron reduction potential of all SOD enzymes is approximately +0.3 V versus NHE, the midpoint of the two half-reactions.[8] Both half-reactions occur thus with the same rate constants, $k_{ox} = k_{red} = \sim 10^9\ M^{-1}\ s^{-1}$.[9–11]

Abbreviations: β, the pyrrolic carbon of the porphyrin ring; *meso*, the 5, 10, 15, or 20 position of the porphyrin ring; Cyt *c*, cytochrome *c*; DMF, *N*,*N*-dimethylformamide; DDQ, 2,3-dichloro-5,6-dicyano-1,4-benzoquinone; $Mn^{III/}Mn^{II}P$, any manganese porphyrin in an oxidized or reduced state (superscripts indicating the manganese oxidation state are often removed for simplicity in the text); MnT-2-PyP$^+$, Mn(III) 5,10,15,20-tetrakis(2-pyridyl)porphyrin; MnT(alkyl)-2-PyP^{5+}, Mn(III) 5,10,15,20-tetrakis(*N*-alkylpyridinium-2-yl)porphyrin where alkyl is methyl (MnTM-2-PyP^{5+}, AEOL10112), ethyl (MnTE-2-PyP^{5+}, AEOL10113) or *n*-hexyl (MnTnHex-2-PyP^{5+}); MnTTEG-2-PyP^{5+}, Mn(III) 5,10,15,20-tetrakis(*N*-(1-(2-(2(-2-methoxyethoxy)ethoxy)ethyl)pyridinium-2-yl)porphyrin; MnTDE-2-ImP^{5+} (AEOL10150), Mn(III) 5,10,15,20-tetrakis(*N*,*N*′-diethylimidazolium-2-yl)porphyrin; MnTPP$^+$, Mn(III) 5,10,15,20-tetraphenylporphyrin; NHE, normal hydrogen electrode; SOD, superoxide dismutase; TFA, trifluoroacetic acid; T-TFA, thallium trifluoroacetate; tris (referring to the buffer), tris(hydroxymethyl)aminomethane.

Keywords: Porphyrin; Porphodimethene; Manganese; Lipophilic; Amphipathic; Cyclic voltammetry; Superoxide dismutase.

* Corresponding authors. Tel.: +1 9196842101; fax +1 9196815851 (I.B.-H.); tel.: +1 9195156406; fax: +1 9195132830 (J.S.L.); e-mail addresses: ibatinic@duke.edu; jlindsey@ncsu.edu

0968-0896/$ - see front matter
doi:10.1016/j.bmc.2007.07.015

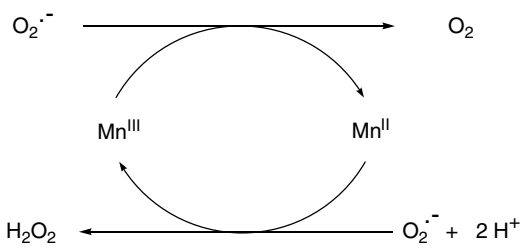

Scheme 1.

The growing appreciation of the role of SOD deficiencies in diverse pathologies has prompted studies of potential therapeutic agents for removing superoxide, preferentially in a catalytic manner. An ideal synthetic SOD mimic should exhibit a redox potential, $E_{1/2}$ of $\sim$ +0.3 V versus NHE. In addition, for optimal performance, the mimic should afford electrostatic facilitation for the dismutation in the same manner as the enzyme itself does.[12] A further requirement concerns bioavailability. In the treatment of central nervous system injuries, such as stroke, for example, the SOD mimic should be able to cross the blood–brain barrier. While some large molecules can cross the blood–brain barrier, in general those molecules that passively cross the blood–brain barrier are amphipathic with molecular weights < 800 Da.[13] In this regard, the use of naturally occurring SOD enzymes as therapeutic agents is unattractive owing to their large size, antigenicity, short circulating half-lives, and cost.

Efforts to construct catalytic SOD mimics for potential therapeutic applications have focused on copper-, iron- or manganese-containing compounds. Manganese is a preferable metal given that manganese, as opposed to iron and copper, does not undergo Fenton chemistry, which results in the formation of the deleterious $^{\cdot}OH$ radical.[1,14] Several different compounds have been studied as potential catalytic SOD mimics, including Mn(III)[12,15–28] and Fe(III)porphyrins,[29–31] organic cyclic nitroxides,[32] Mn(II) complexes with pentaazacyclodecane ligands (manganese cyclic polyamines),[33,34] and Mn(III) salen complexes.[35,36] Recently, given the key importance of the mitochondria in a number of diseases, compounds targeting mitochondria have been increasingly sought. Examples include a lipophilic triphenylphosphonium cation attached to coenzyme Q via an alkyl linker,[37] carboxypropyl nitroxide linked to triphenylphosphonium ion,[38] and the manganese chelate of a *tetra*-pyridinium porphyrin (Mn^{III}TM-4-PyP^{5+}) that contains a mitochondrial targeting peptide.[39] Most of the SOD mimics are also able to decrease the level of reactive species other than $O_2^{\cdot -}$.[17–19,23,26,29–32,40] However, exceptions include Mn(II) cyclic polyamines,[33,34] which are reportedly $O_2^{\cdot -}$ specific, due to the inability of the pentacoordinated divalent manganese to further coordinate $ONOO^-$. Synthetic catalytic SOD mimics in principle can be tuned in a variety of ways for tissue targeting, activity, and stability. Of the various molecular architectures that have been investigated to date, manganese porphyrins appear the most suitable due to the high metal-ligand stability and broad range of possibilities for modifying the core porphyrin ligand so as to alter the metal-centered redox potential, charge, and lipophilicity.

Thus far we have extensively studied hydrophilic manganese porphyrins.[12,17,19–28] Examples are shown in Chart 1 along with their catalytic rate constants for $O_2^{\cdot -}$ dismutation. A number of key findings emerged. With electron-withdrawing, cationic, quaternized *ortho* heterocyclic (e.g., pyridyl) groups at the *meso* positions, both favorable $E_{1/2}$ and electrostatics are achieved, resulting in compounds that are only a few-fold less potent in vitro than the SOD enzyme itself.[22,25] Moreover, the *ortho* isomers are bulkier than their *para*-substituted analogues[15,16,18] and thus do not interact significantly with nucleic acids which make them less toxic.[17] The ability to scavenge $O_2^{\cdot -}$ paralleled the ability to reduce peroxynitrite.[19,23,26] Upon decreasing the levels of reactive species, the manganese porphyrins can finely modulate signaling pathways by inactivating transcription factors HIF-1α, NF-κB, and AP-1.[41–43] Several porphyrins of that series were effective in ameliorating oxidative stress injuries in vivo as well. It was also found that the lack of charges close to the metal site, despite a favor-

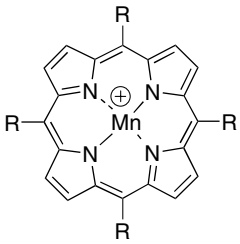

R	Compound	log k_{cat}
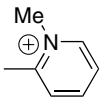	MnTM-2-PyP^{5+}	7.79
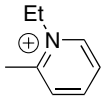	MnTE-2-PyP^{5+}	7.76
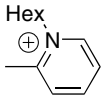	MnTnHex-2-PyP^{5+}	7.79
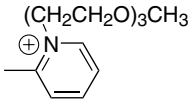	MnTTEG-2-PyP^{5+}	8.11
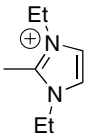	MnTDE-2-ImP^{5+}	7.48

Chart 1. Water-soluble manganese porphyrin-based SOD mimics and their rate constants for superoxide dismutation.

able $E_{1/2}$, greatly diminished the $O_2^{\cdot-}$ scavenging ability: while having the same $E_{1/2}$ values, MnTE-2-PyP^{5+} is ~ 130-fold more potent in dismuting $O_2^{\cdot-}$ than the singly charged analogue MnBr$_8$T-2-PyP$^+$.[12] The porphyrin MnTE-2-PyP^{5+} entered the mouse mitochondria despite excessive hydrophilicity.[28] Such data complement a study with submitochondrial particles indicating that at ⩾ 3 μM, MnTE-2-PyP^{5+} would protect mitochondria from ONOO$^-$-mediated damage.[18] Preliminary pharmacokinetic data show that MnTE-2-PyP^{5+} enters the brain as well, though at significantly lower levels than other organs such as the liver and kidneys.[44]

Therefore, efforts were recently made to design more bioavailable compounds, that is, compounds with higher lipophilicity that can cross the blood–brain barrier at significant levels and have longer blood-circulating half-lives.[25] The 2-alkylpyridyl compound bearing hexyl chains, MnTnHex-2-PyP^{5+}, is several fold more lipophilic than MnTE-2-PyP^{5+}, and is > 10-fold more effective in protecting SOD-deficient *Escherichia coli* when grown aerobically, despite identical antioxidant potency.[45] Furthermore, in a renal model of ischemia/reperfusion, a single dose of 50 μg/kg offered protection against renal dysfunction, ATP depletion, MnSOD inactivation and nitrotyrosine formation.[27] Such data indicate that compounds that display higher lipophilicity may be more suitable for in vivo use, particularly when targeting lipophilic environments/organs such as membranes and the central nervous system.

Herein, we describe the synthesis of a collection of stable manganese porphyrins that bear diverse substituents in order to tune the redox properties of the metal site and to preferentially target lipophilic cellular components such as membranes. Some of the compounds have sufficiently high $E_{1/2}$ to allow $O_2^{\cdot-}$ dismutation on the basis of thermodynamic considerations. Compounds targeting lipids may not provide electrostatic facilitation for the reaction with negatively charged reactive species. However, the potential for the reduction of oxygen is shifted in an aprotic environment (e.g., in DMF the $E_{1/2}$ of $O_2/O_2^{\cdot-} = -600$ mV vs NHE). Thus, in a lipid environment, a Mn^{III}P without electrostatic facilitation may still be able to effectively oxidize $O_2^{\cdot-}$ to yield O_2 and the corresponding Mn^{II}P (where 'P' denotes a porphyrin). Such compounds should enable studies of the scavenging of reactive oxygen species within cellular lipid compartments to suppress the deleterious consequences of lipid peroxidation.

2. Results and discussion

2.1. Molecular design

Our design of *meso*-substituted manganese porphyrin-based SOD mimics includes one or both of the following features: (i) electron-withdrawing substituents, (ii) lipophilic substituents to facilitate crossing of lipid bilayer membranes and ultimately the blood–brain barrier. The prototypical target molecules are shown in Chart 2. The substituents are arranged in patterns ranging from the traditional A$_4$-porphyrins (which have been predominantly used in prior SOD designs) to architectures of lower symmetry including A$_3$B-, *trans*-A$_2$B$_2$-, *trans*-AB$_2$C-, *trans*-A$_2$-, *trans*-A$_2$B-, and *cis*/*trans*-A$_2$B-porphyrins. None of the target compounds possess β-substituents. The presence of substituents at both *meso*- and β-positions may cause ruffling of the ring and thereby increase demetalation.

The electron-withdrawing substituents attached to the porphyrin core are employed to shift the potential to the desirable range (+0.3 V vs NHE). Examination of the one-electron reduction potential of each member of a set of free base porphyrins bearing diverse *meso*-substituents has led to the determination of 'partial potential values,' which assess the shifts in potential characteristic of a substituent.[46–48] While knowledge of such shifts is useful in guiding the design of the porphyrin molecules, a complete set of potentials for the substituents of interest here was not available. Established partial potential values of relevant groups for this study are as follows: methyl (−15 mV), phenyl (+26 mV), and pentafluorophenyl (+114 mV).[48] In addition, the mono-*meso* nitration of etioporphine and octaethylporphyrin resulted in a +500 and +340 mV shift, respectively, of the reduction potential of the porphyrin macrocycle.[49,50] For the octaethylporphyrin, the potential shifted linearly up to the introduction of the third *meso*-nitro group.[49] The effect of a substituent in a *meso* position is usually more pronounced than that of the same substituent in a β position.[51] It should also be noted that although the presence of a redox-active metal center might limit the predictive utility of partial potential values by shifting the redox site from a ligand-based to metal-based process,[46] a qualitatively similar trend on the overall substituent effect is still generally expected.

We sought to use *meso*-benzoyl or *meso*-trifluoromethyl groups because of their strong electron-withdrawing properties (Chart 2, **Mn-1** to **Mn-4**). The manganese isoporphodimethene (**Mn-5**) was attractive to probe the role of macrocycle aromaticity. The effects of *meso*-oxo or *meso*-pentafluorophenyl substituents on the redox potential were also investigated (**Mn-6**, **Mn-7**, and **Mn-8**). The manganese porphyrins **Mn-9**, **Mn-13**, and **Mn-14** were designed to locate at the interior of bilayer lipid membranes. We also designed molecules to study the effect of the nitro group on the reduction potential (**Mn-10**, **Mn-11**, **Mn-12**, and **Mn-14**). Finally, the manganese porphyrin **Mn-15** is amphipathic and may potentially cross the blood–brain barrier.

A number of the compounds contain trifluoromethyl groups. The trifluoromethyl group is an attractive substituent for several reasons: (1) lipophilicity, (2) electron-withdrawing effect, and (3) small size, thus keeping the interfacial cross-sectional area low. The installation of a trifluoromethyl group has yielded beneficial results on a range of medicinal agents. For example, a trifluoromethyl-epothilone derivative has resulted in a decrease in toxicity and a broader therapeutic index.[52,53] Some taxoids bearing a trifluoromethyl or difluoromethyl groups showed higher

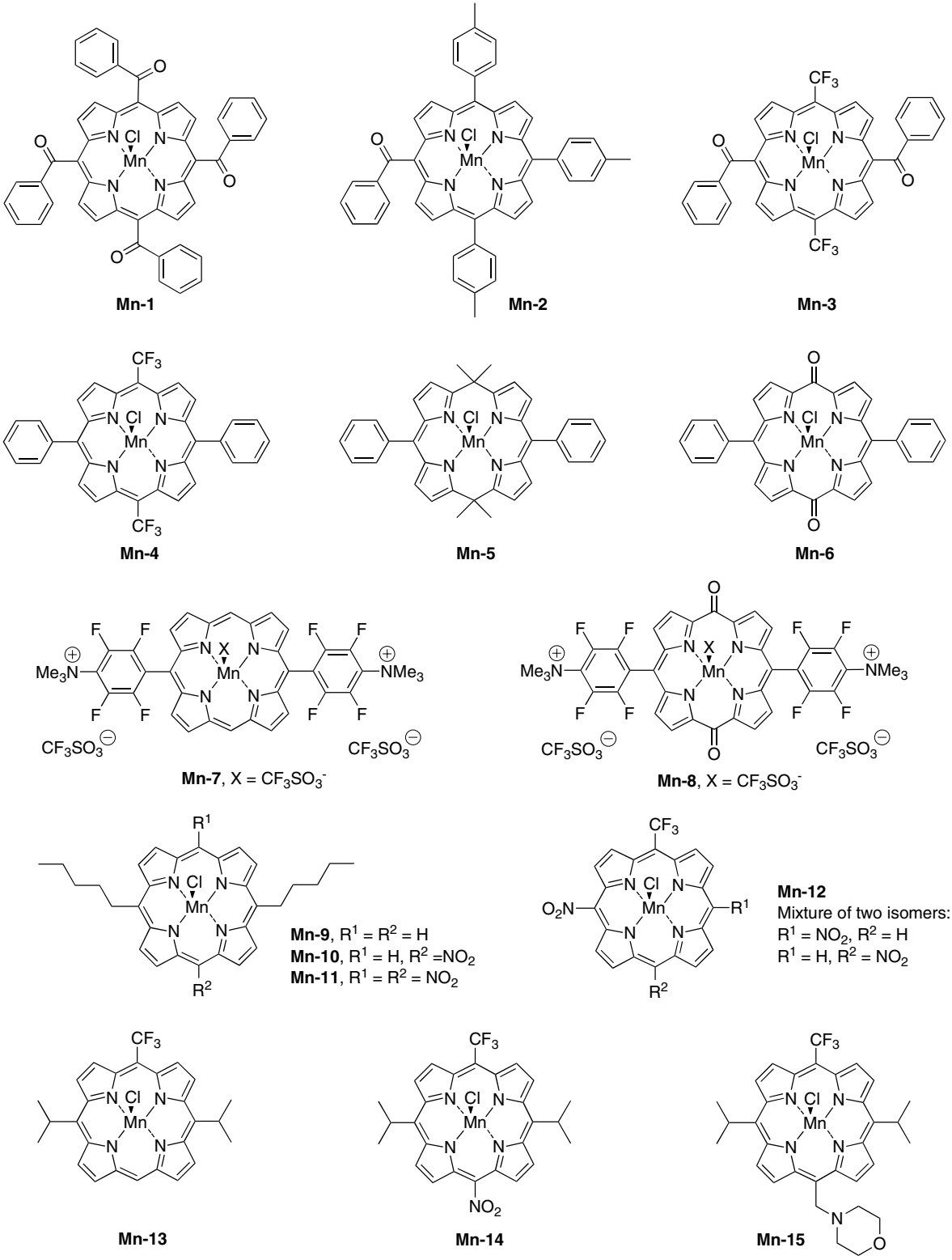

Chart 2.

potency than their non-fluorinated counterparts against certain cancer lines and acted as versatile probes for biomedical problems.[54] The photosensitizing efficacy of purpurinimides and bacteriopurpurinimides also was enhanced by the introduction of trifluoromethyl substituents.[55]

2.2. Synthesis

The free base porphyrins were prepared using two rational methodologies: (1) reaction between a dipyrromethane and an aldehyde to give the corresponding *trans*-A_2- or *trans*-A_2B_2-porphyrin;[56] and (2) acylation

or alkylation of a dipyrromethane at the 1,9-positions followed by condensation of the dipyrromethane derivative with a dipyrromethane to give the corresponding A- or *trans*-AB_2C-porphyrin.[57] Three dipyrromethanes were used herein (**16**,[58,59] **17**,[59] and **18**[60]), all of which are known compounds.

Two literature methods were employed for manganese insertion, which differed only in the reaction conditions. The first method (method A) entailed treatment of the free base porphyrin with $MnCl_2$ and 2,6-lutidine in chloroform/methanol with mild heating (Eq. 1).[61] The second method (method B) entailed treatment of the free base porphyrin with $MnCl_2$ in refluxing DMF (Eq. 1).[62]

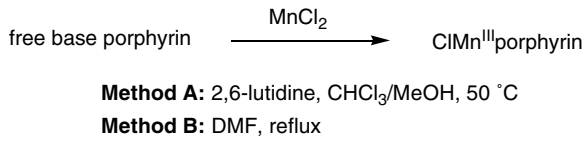

(1)

2.2.1. Porphyrins bearing benzoyl and/or trifluoromethyl groups. The *meso*-benzoyl and *meso*-trifluoromethyl groups were anticipated to provide strong electron-withdrawing effects. The tetrabenzoylporphyrin **1**,[63] mono-benzoylporphyrin **2**,[63] dibenzoyl-bis(trifluoromethyl)porphyrin **3**,[60] and bis(trifluoromethyl)porphyrin **4**[60] were prepared by known procedures. Manganese metalation (via method A) of each free base porphyrin **1**–**4** afforded the corresponding manganese chelates **Mn-1**, **Mn-2**, **Mn-3**, and **Mn-4** in good yields.

2.2.2. Porphodimethenes and oxoporphodimethenes. Porphodimethenes[64–67] lie at the interface between calix[4]pyrroles and porphyrin chemistry. The non-aromatic macrocycle provided by the porphodimethene was of interest for fundamental studies of SOD activity.

Three syntheses of porphodimethene **5** have been reported and proceed as follows: (1) condensation of 5-phenyldipyrromethane, pyrrole, and acetone in the presence of TFA followed by oxidation with DDQ (5% yield);[66] (2) condensation of 5,5-dimethyldipyrromethane (**16**), 5-phenyldipyrromethane and benzaldehyde in the presence of $BF_3{\cdot}OEt_2$ followed by oxidation with DDQ (9% yield);[68] and (3) 1-acylation of 5,5-dimethyldipyrromethane followed by reduction and self-condensation.[69]

We carried out the synthesis of porphodimethene **5** by the '2 + 2' condensation of 5,5-dimethyldipyrromethane (**16**) and benzaldehyde. Thus, treatment of dipyrromethane **16** with benzaldehyde in the presence of TFA followed by oxidation with DDQ afforded **5** in 10% yield (Scheme 2). Metalation of **5** with $MnCl_2$ in DMF (via method B) gave **Mn-5** in 83% yield (crystallographic data are given in the Supporting Information). The manganese insertion of **5** was carried out using a large excess (up to 53 equiv) of the metal ion and was slower than the metal insertion of dioxoporphodimethenes or porphyrins. The sluggish metal insertion may be due to steric hindrance from the axial methyl groups at the

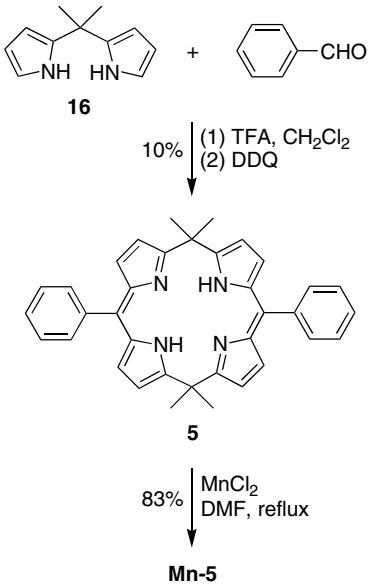

Scheme 2.

meso-positions and the basicity of the nitrogens, resulting from the non-aromatic character of **5**.

The condensation of dipyrromethane (**17**) and benzaldehyde following a literature method[70] afforded 5,15-diphenylporphyrin (**19**). Oxygenation of **19** with thallium trifluoroacetate (TTFA) afforded the thallium complex of 5,15-dioxo-10,20-diphenylporphodimethene (Scheme 3).[71] An excess of TTFA (18 equiv) was employed because larger amounts of byproducts were formed upon extended reaction with a stoichiometric amount of

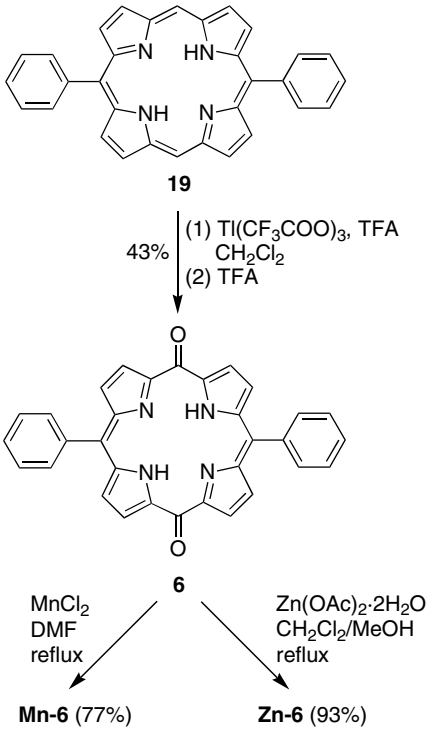

Scheme 3.

TTFA. In an early report by Smith et al. for the preparation of octaethyldioxoporphodimethene,[71] SO_2 gas was bubbled into the reaction mixture to reduce Tl(III) to Tl(I) for demetalation. Treatment of **19** with the same procedure afforded a black precipitate, which upon LD–MS analysis showed the desired compound **6**, the thallium salt of **6** and higher molecular weight materials corresponding to dimeric and other polymeric products of **6**. The dimerization of radical ion intermediates has been reported for other dioxoporphodimethenes.[72] To minimize possible side reactions, the crude thallium salt was demetalated with TFA, and the dioxoporphodimethene **6** was isolated in 43% yield after column chromatography. Metalation of **6** with $MnCl_2$ in DMF (via method B) afforded **Mn-6** in 77% yield. Metalation of **6** with $Zn(OAc)_2{\cdot}2H_2O$ afforded **Zn-6** in 93% yield. The synthesis of a cationic oxoporphodimethene (**Mn-8**) is discussed in the next section.

2.2.3. Tetrafluorotrimethylanilinium-substituted porphyrins. Tetrafluorotrimethylanilinium substituents were introduced for their electron-withdrawing properties and as a potential means of accelerating reaction with superoxide by electrostatic interaction. Only two cationic substituents were attached to the porphyrin core to limit the molecular size and aqueous solubility of the complex.

The condensation of dipyrromethane **17** and pentafluorobenzaldehyde in the presence of $BF_3{\cdot}O(Et)_2$ in $CHCl_3$ (BF_3-ethanol cocatalysis)[73] gave porphyrin **20**. Kadish et al. have reported that heating tetrakis(pentafluorophenyl)porphyrin in DMF affords the dimethylamino-substituted porphyrin.[74] Later studies by Richards and Miskelly have shown that the presence of $HN(CH_3)_2{\cdot}HCl$ is beneficial for this substitution reaction.[75] The substitution of the *para*-fluoro groups of **20** with dimethylamino groups was carried out in the presence of excess $HN(CH_3)_2{\cdot}HCl$ in DMF at 120 °C for 24 h to yield 5,15-bis(2,3,5,6-tetrafluoro-4-dimethylaminophenyl)porphyrin (**21**) in 78% yield (Scheme 4). Metalation of **21** with $MnCl_2$ in DMF (via method B) gave **Mn-21**. Methylation[75] of **Mn-21** upon treatment with methyl triflate in $(CH_3O)_3PO$ afforded the tricationic manganese complex **Mn-7** in 52% yield (on the assumption that the counterion is triflate). On the basis of the elemental analysis data, which were consistent with the presence of the porphyrin complex, one molecule of trimethyl phosphate, and one molecule of water, the corrected yield of the porphyrin complex itself would be 45%.

The oxygenation of porphyrin **20** using TTFA in TFA at room temperature followed by demetalation with TFA gave dioxoporphyrin **22**.[71] The reaction was worked up after 40 min, because extended reaction times gave byproducts and decreased the yield of **22**. Oxoporphodimethene **23** was synthesized in 57% yield from **22** following a strategy similar to that used for the synthesis of **21** (Scheme 5) (crystallographic data for **23** are given in the Supporting Information). Metalation of **23** (via method B) followed by methylation using methyl triflate[75] afforded manganese porphyrin **Mn-8** in 67% yield (on the assumption that the counterion is triflate). On the basis of the elemental analysis data, which were consistent with the presence of the porphyrin complex and two molecules of trimethyl phosphate, the corrected yield of the porphyrin complex itself would be 55%.

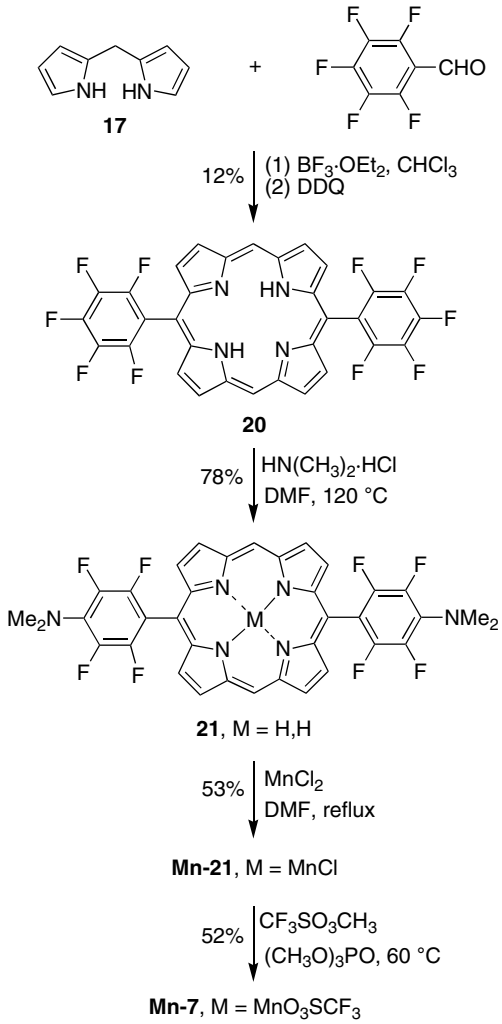

Scheme 4.

Compound **Mn-8** was found to display three electrochemical waves (vide infra), which were attributed to both the quinone moiety and the manganese ion. The zinc chelate analogue of **Mn-8** (**Zn-8**) was synthesized as a model compound for cyclic voltammetry experiments. Given that zinc porphyrins do not undergo metal-centered redox chemistry, the zinc chelate analogue would enable assignment of the electrochemical waves corresponding to the quinone moiety, and thus, by elimination, the waves corresponding to the manganese center in **Mn-8**. Reaction of the free base **23** with $Zn(OAc)_2$ generated the zinc complex **Zn-23** in 85% yield. Quaternization of **Zn-23**, employing a strategy similar to the one used for the synthesis of **Mn-8**, afforded compound **Zn-8** in 73% yield (Scheme 5).

2.2.4. Pentyl-substituted porphyrins and nitroporphyrins. Two alkyl chains were introduced on the porphyrin core to increase the lipophilicity of the complex as required to

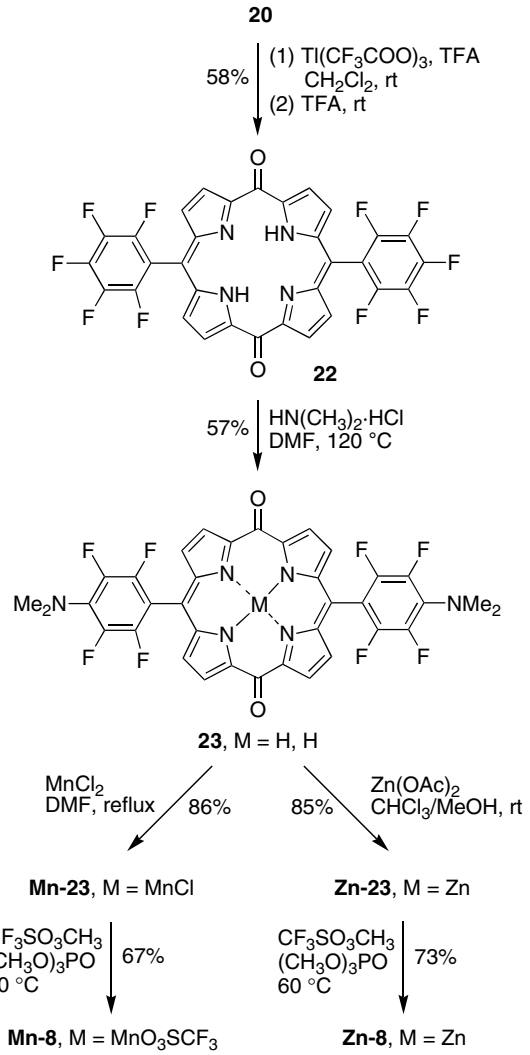

Scheme 5.

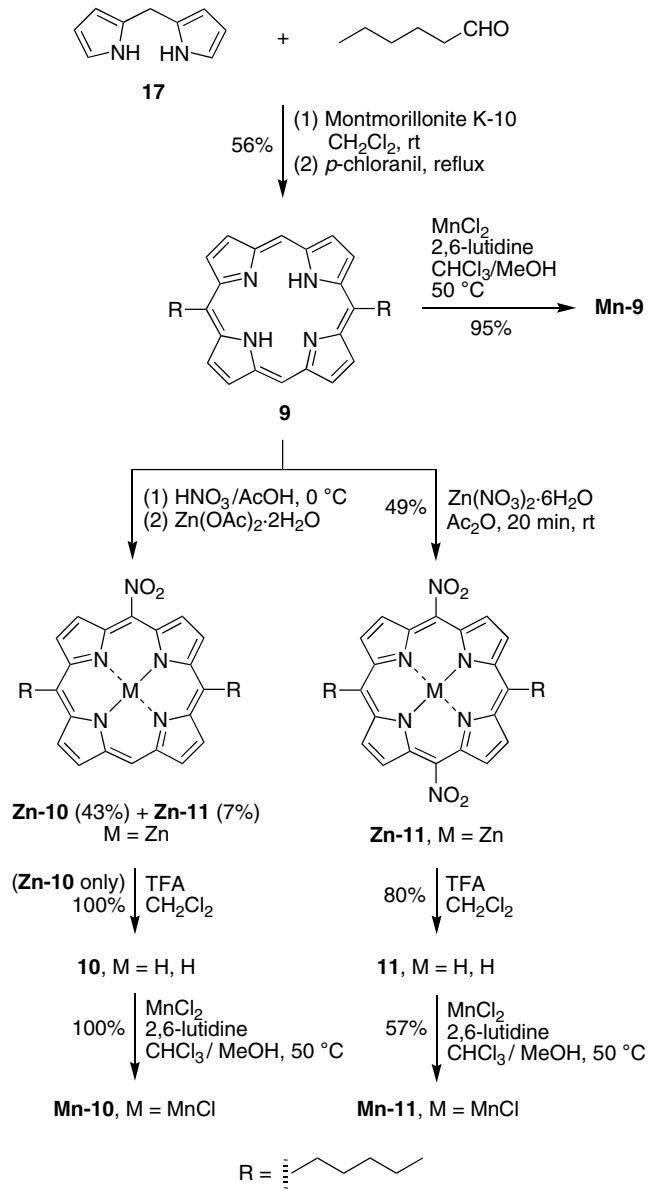

Scheme 6.

improve the permeation of cell membranes. Pentyl chains were employed to impart enough lipophilicity while limiting the toxicity previously observed with longer alkyl chains.[45]

The synthesis of alkyl-substituted *trans*-A_2-porphyrins has been reported. For example, the condensation of heptanal with dipyrromethane in dichloromethane under acidic conditions followed by oxidation with DDQ generated the corresponding *trans*-A_2-porphyrin in 27% yield.[76] Here, the condensation of hexanal and dipyrromethane (**17**)[59] in the presence of clay (Montmorillonite K-10) gave porphyrin **9** in 56% yield (Scheme 6) after only a single column chromatography purification and without any scrambling. Metalation of **9** using method A gave **Mn-9** in 95% yield.

Nitro groups were then introduced because of their ability to shift the redox potentials to more positive values. Nitration of porphyrin **9** was achieved with fuming nitric acid in glacial acetic acid[77] at 0 °C for 20 min to afford an inseparable mixture of mononitroporphyrin **10** and dinitroporphyrin **11** in a 6:1 ratio. Zinc metalation enabled separation of the mono- and dinitro-porphyrins (**Zn-10** and **Zn-11**, respectively) by silica chromatography (Scheme 6). The facile separation of the zinc derivatives prompted us to use zinc nitrate[78] as the nitrating agent. Nitration under these conditions led exclusively to zinc(II)-5,15-di-*n*-pentyl-10,20-dinitroporphyrin (**Zn-11**) in 49% yield. Demetalation of **Zn-10** or **Zn-11** in TFA gave **10** or **11**. Manganese insertion of **10** or **11** with $MnCl_2$ and 2,6-lutidine afforded manganese porphyrin **Mn-10** or **Mn-11** in 100% or 57% yield, respectively.

2.2.5. Porphyrins bearing nitro and trifluoromethyl groups. 1,9-Diformyldipyrromethane **24** was synthesized according to a literature method.[79] Reduction of **24** with $NaBH_4$ gave dipyrromethane-1,9-dicarbinol **24-diol**. The acid-catalyzed condensation of **24-diol** and dipyrromethane **17** gave porphyrin **25** in 8% yield (Scheme 7). Porphyrin **25** was treated with $Zn(NO_3)_2{\cdot}6H_2O$ in acetic anhydride to afford the Zn-dinitroporphyrin **Zn-12**.

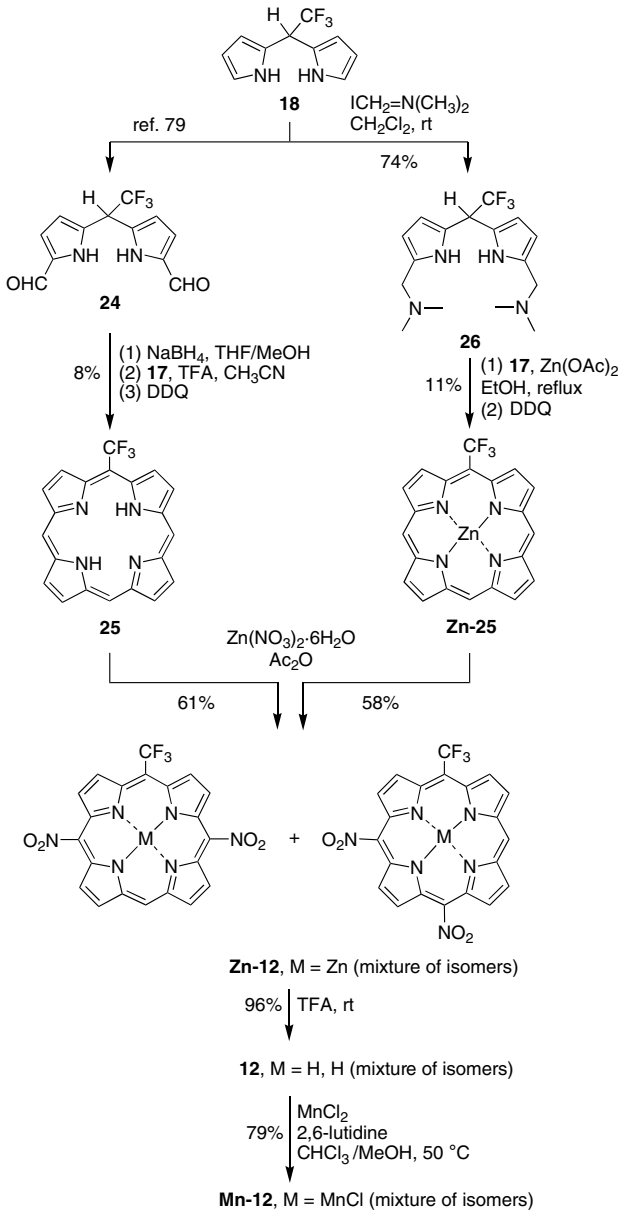

Scheme 7.

An alternative route to compound **Zn-12** is possible via the method developed by Fan et al.[80] Treatment of 5-(trifluoromethyl)dipyrromethane (**18**) with Eschenmoser's salt furnished the 1,9-bis(*N*,*N*-dimethylaminomethyl)dipyrromethane **26** in 74% yield and > 95% purity (as determined by ^{1}H NMR analysis) after simple aqueous-organic work up. Treatment of **26** with dipyrromethane (**17**) in refluxing ethanol in the presence of $Zn(OAc)_2$ followed by oxidation with DDQ afforded porphyrin **Zn-25** in 11% yield after column chromatography. The reaction of **Zn-25** with $Zn(NO_3)_2{\cdot}6H_2O$ and acetic anhydride under the same conditions as for the free base porphyrin **25** yielded the dinitro derivative **Zn-12**.

The latter route for the synthesis of **Zn-12** is superior to the one utilizing the 1,9-diformyldipyrromethane **24**,[79] as **26** displays improved reactivity versus **24-diol** in the porphyrin-forming reaction. Furthermore, although **24** and **26** are obtained in similar yields (a 79% yield is reported for **24**), the synthesis of **26** requires neither chromatographic purification nor recrystallization as for **24**, therefore simplifying the procedure. Although this procedure affords the Zn-chelate of **25**, the central metal did not cause any problems in the subsequent step.

The nitration of **Zn-25** proceeded without much regioselectivity, yielding a 2:1 mixture of *cis* and *trans* isomers as determined by ^{1}H NMR analysis. The separation of these two isomers was not possible by column chromatography; therefore, the mixture was carried forward to the next step. Porphyrin **Zn-12** was demetalated with TFA to give free base porphyrin **12**, which upon metalation (via method A) afforded **Mn-12** in 79% yield.

2.2.6. Porphyrins bearing isopropyl and trifluoromethyl groups. With a view to synthesize lipophilic or amphipathic manganese porphyrins with tuned reduction potentials, we focused on introducing isopropyl groups (to provide lipid solubility) and trifluoromethyl groups (to shift the reduction potential). The 1,9-diacylation of **18** with EtMgBr and isobutyroyl chloride afforded 1,9-diacyldipyrromethane **27**. Reduction of **27** using $NaBH_4$ gave the dipyrromethane-1,9-dicarbinol **27-diol**. The standard acid-catalyzed condensation[57] of **27-diol** with dipyrromethane **17** gave **13** in 16% yield (Scheme 8). Metalation of **13** (via method A) afforded manganese porphyrin **Mn-13** in 76% yield.

Treatment of porphyrin **13** with 1 equivalent of $Zn(NO_3)_2{\cdot}6H_2O$ in $CHCl_3$/acetic anhydride (2:1) afforded **Zn-14** in 32% yield (Scheme 8). Demetalation of **Zn-14** using TFA afforded free base porphyrin **14**, which upon metalation (via method A) afforded manganese porphyrin **Mn-14** in 82% yield.

Compound **Mn-15** was designed to target the blood–brain barrier. The key structural determinants for passive diffusion across the blood–brain barrier are more restrictive than those for other cellular membranes. The constraints are generally found to be as follows:[81] (1) a cross-sectional area at the hydrophilic/hydrophobic interface of < 50 Å^2, (2) pK_a for acids > 4, and (3) pK_a < 10 for bases. Very hydrophobic drugs with cross-sectional areas ⩾ 80 Å^2 generally do not cross the blood–brain barrier. Thus amphiphilic molecules with modest interfacial cross-sectional areas and bearing neither strong acids nor bases have the highest propensity to cross the blood–brain barrier.[81] Thus, the features of **Mn-15** include (1) the use of polar and hydrophobic groups, (2) an electron-withdrawing substituent to tune the potential, (3) overall low molecular weight, (4) no *meso*-aryl groups, which increase the cross-sectional area thereby impeding membrane permeability, and (5) no strongly acidic or basic substituents. The morpholine substituent was chosen as it is present in a pyrrole-pyrimidine antioxidant (not an SOD mimic) that crosses the blood–brain barrier,[82] and is also found in a variety of tricyclic antidepressants and other neuroactive therapeutic agents including reboxetine.[83]

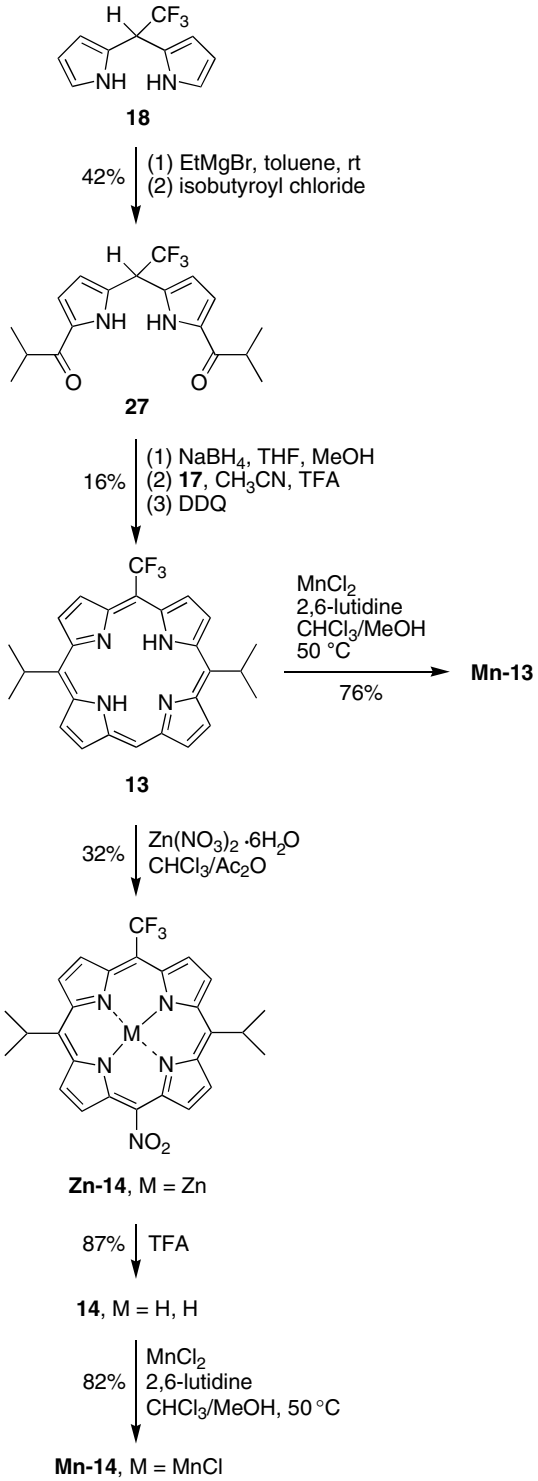

Scheme 8.

Exploratory studies showed that it would be difficult to synthesize an aminomethyl-substituted porphyrin by condensation of a dipyrromethane-dicarbinol derived from **27** with a 5-amino-substituted dipyrromethane. Therefore, we decided to introduce a formyl group first and then transform the formyl group into the morpholinomethyl group by reductive amination.

We synthesized the required formylporphyrin **28** following standard literature methods for copper insertion, formylation, and subsequent demetalation (Scheme 9). Porphyrin **13** was metalated with copper using $Cu(OAc)_2{\cdot}H_2O$ in $CHCl_3$-methanol to afford **Cu-13**.[84] Vilsmeier formylation[84] of **Cu-13** gave the formylporphyrin **Cu-28**, which upon demetalation[84] in TFA containing concentrated H_2SO_4 furnished the formylporphyrin **28**. The reductive amination of **28** with morpholine and sodium cyanoborohydride in dichloromethane/methanol[85] afforded the target porphyrin **15** along with the

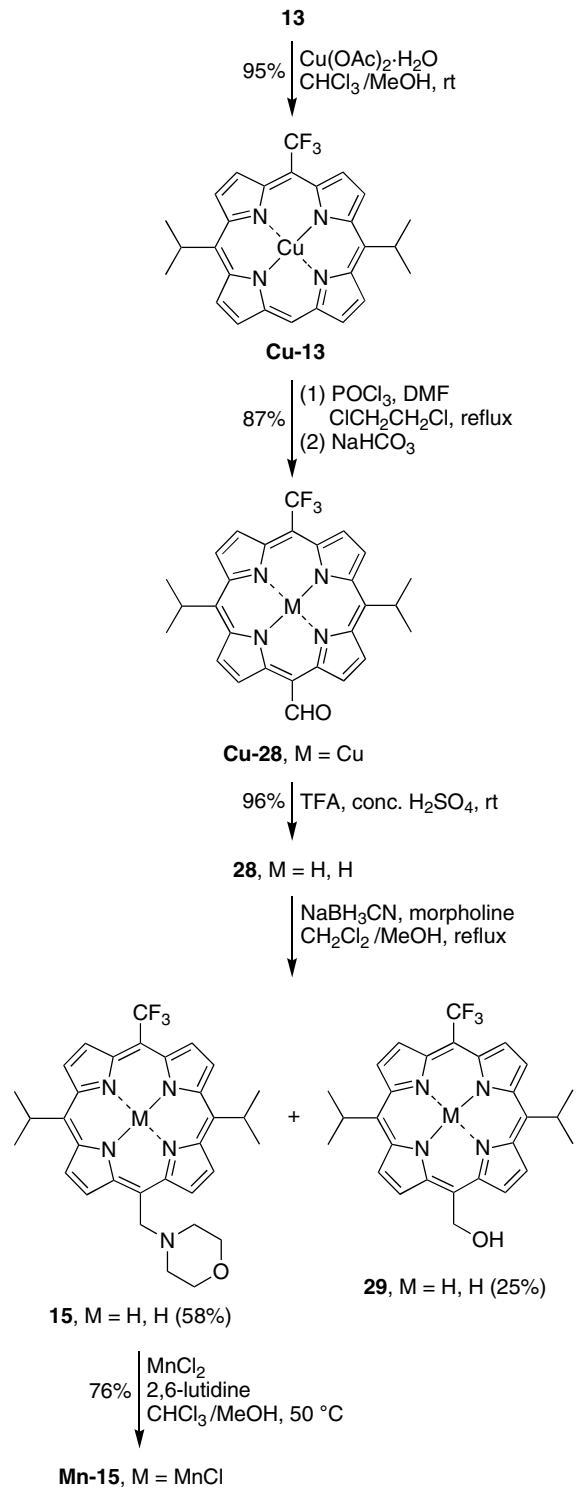

Scheme 9.

byproduct hydroxymethyl-porphyrin **29**. The two porphyrins **15** (58%) and **29** (25%) were separated by chromatography on alumina. Metalation of free base porphyrin **15** (via method A) afforded manganese porphyrin **Mn-15** in 76% yield.

Attempts to shift the reduction potential of metal chelates (Zn, Cu) of **15** by treatment with *N*-chlorosuccinimide in refluxing methanol[86] or CoF_3 in dichloromethane[87] did not provide the required product. Similar attempts to chlorinate, acylate,[84] or nitrate **Cu-28** or **Zn-28** also were unsuccessful. We attribute the failures to functionalize the porphyrins **Cu-28** and **Zn-28** to the presence of the labile formyl group.

2.2.7. Chemical characterization. Each free base porphyrin was characterized by absorption spectroscopy, ^{1}H NMR spectroscopy, laser desorption mass spectrometry (LD–MS), and high-resolution FAB-MS, except free base porphyrin **12** due to poor solubility. The manganese porphyrins were characterized by absorption spectroscopy, fluorescence spectroscopy, LD–MS (or ESI-MS), and high-resolution FAB-MS. ^{1}H NMR spectroscopy was not performed on the manganese porphyrins owing to the paramagnetic character of the manganese ion. The structures of both the manganese porphodimethene complex **Mn-5** and the free base dioxoporphodimethene **23** were investigated by X-ray crystallography. The ORTEP diagrams of **Mn-5** and **23**, along with selected bond distances and bond angles for both structures, are given in the Supporting Information.

2.2.8. Solubility. All manganese porphyrins examined herein are soluble in methanol, other than **Mn-1**, which is soluble in DMF. Compound **Mn-1** was examined for lipophilicity by the well-established method of partitioning between *n*-octanol and water (where **Mn-1** was first dissolved in *n*-octanol and then water was added). **Mn-1** was soluble in *n*-octanol and did not distribute into the aqueous layer. Comparable behavior is expected for all the other neutral manganese porphyrins described herein. On the other hand, **Mn-7** and **Mn-8** bear charged substituents and are water-soluble. Accordingly, **Mn-7** and **Mn-8** were first dissolved in water and then *n*-octanol was added. Both compounds were distributed essentially entirely in the aqueous layer with none in the *n*-octanol phase.

2.3. Electrochemistry

The redox potentials of the manganese porphyrins synthesized were determined to assess the effects of substituents. The metal-centered reduction potentials, $E_{1/2}$, of all of the new manganese porphyrins were measured versus Ag/AgCl in a mixture of methanol/H_2O (or in DMF/H_2O in the case of **Mn-1**). The values determined under these conditions and the corrected ones for an aqueous system versus NHE are gathered in Table 1. The corrected values were obtained by adding 96 mV or 28 mV to the potentials determined versus Ag/AgCl in MeOH/H_2O or DMF/H_2O, respectively.

Table 1. Metal-centered redox potentials, $E_{1/2}$ for $Mn^{III}P/Mn^{II}P$ redox couple of manganese porphyrins

Compound	$E_{1/2}$ versus Ag/AgCl[a] (V)	$E_{1/2}$ versus NHE[b] (V)
Mn-1[c]	+0.060	+0.088
Mn-2	−0.327	−0.231
Mn-3	−0.052	+0.044
Mn-4	−0.190	−0.094
Mn-5	−0.265	−0.169
Mn-6	−0.013	+0.082
Mn-7	−0.216	−0.120
Mn-8	+0.353	+0.449
Mn-9	−0.450	−0.354
Mn-10	−0.249	−0.153
Mn-11	−0.039	+0.057
Mn-12	+0.112	+0.208
Mn-13	−0.393	−0.297
Mn-14	−0.195	−0.099
Mn-15	−0.442	−0.346
Zn-8[d]	+0.100	+0.196
	−0.213	−0.117
Mn-TE-2-PyP^{5+}	+0.132	+0.228
Mn-TE-2-PyP^{5+}[c]	+0.200	+0.228
Mn-TM-2-PyP^{5+}	+0.126 (−0.041)[e]	+0.220
Ferrocenemethanol	+0.385 (+0.218)[e]	
Ferrocene	+0.379	

[a] $E_{1/2}$ was measured in MeOH/H_2O (9:1) containing 0.05 M tris buffer and 0.1 M NaCl at pH 7.8.
[b] Corresponding corrected values for an aqueous system versus NHE.
[c] $E_{1/2}$ was measured in DMF/H_2O (9:1) containing 0.05 M tris buffer and 0.1 M NaCl at pH 7.8.
[d] Non-metal centered redox couples.
[e] MnTM-2-PyP^{5+} and ferrocenemethanol were measured in the following media: MeOH/H_2O (9:1), 0.1 M NaCl, 0.05 M tris buffer, pH 7.8; and H_2O, 0.1 M NaCl, 0.05 M tris buffer, pH 7.8 (value in parentheses). An identical shift in potential (167 mV) upon changing from MeOH/H_2O to the aqueous system was observed with both ferrocenemethanol and MnTM-2-PyP^{5+}.

The electrochemical waves could be easily assigned except in the case of **Mn-6** and **Mn-8**. Compound **Mn-8** exhibited three redox couples: +0.449 V, +0.100 V and −0.342 V versus NHE. The zinc analogue **Zn-8** only had two such couples, at +0.196 V and −0.117 V versus NHE. Thus, the most positive $E_{1/2}$ of **Mn-8** was attributed to the metal site, as it was absent from the voltammogram of **Zn-8** (zinc porphyrins do not undergo metal-centered electrochemistry). Compound **Mn-6** has a structure similar to that of **Mn-8** and also exhibited three redox couples at +0.082 V, −0.167 V and −0.357 V versus NHE; however, all were irreversible. By analogy of **Mn-6** with **Mn-8**, the most positive potential was assigned as the metal-centered potential. The other electrochemical waves observed probably result from the reduction of the *meso*-oxo substituents to produce semiquinone and quinol species.

A potential of −0.231 V versus NHE was found for **Mn-2**. This value is slightly more positive than the potentials for MnTPP$^+$ and MnT-2-PyP$^+$, previously measured to be −0.270 V and −0.280 V versus NHE, respectively.[88] This effect results from the electron-withdrawing properties of the benzoyl substituent. This effect is further increased when all four *meso* positions are substituted

with benzoyl groups (**Mn-1**), the potential then shifting to a positive value (+0.088 V vs NHE). The replacement of two benzoyl groups of **Mn-1** with two CF_3 groups (**Mn-3**) decreases the potential slightly. This phenomenon may result from a weaker electron-withdrawing ability of the trifluoromethyl substituent compared to the benzoyl group. With two CF_3 and two phenyl groups in a *trans*-A_2B_2 configuration, a negative shift of −138 mV is observed for the $E_{1/2}$ of **Mn-4** relative to **Mn-3**. This indicates that the partial potential for a benzoyl substituent is much larger than that for a phenyl group. Yet, the presence of two *meso*-oxo substituents in **Mn-6**, instead of two CF_3 groups in **Mn-4**, causes a large positive shift in the potential (+176 mV).

The nonaromatic porphodimethene **Mn-5** has a redox potential similar to the potential of manganese ligated to a nonaromatic manganese salen ($E_{1/2}$ = −130 mV vs NHE).[89] The lack of full conjugation in **Mn-5** results in a destabilization of the Mn^{+3} oxidation state as reflected by the comparable more positive reduction potential of **Mn-5** with respect to that of $MnTPP^+$ (−0.270 V vs NHE).

As expected, **Mn-7**, with only two tetrafluorotrimethylanilinium groups attached in the *meso* positions, displays a more negative potential (−0.120 V vs NHE) compared to the fully substituted analogue (+0.060 V vs NHE).[88] Introduction of oxo substituents in the remaining two *meso* positions resulted in a significant shift of +569 mV of the potential (**Mn-8**). The effect of oxo substituents is thus the largest upon combination with the electron-withdrawing tetrafluorotrimethylanilinium moieties in the other two *meso* positions (**Mn-8**).

The introduction of one electron-withdrawing nitro substituent to the dipentylporphyrin **Mn-9** resulted in a shift of about +200 mV (**Mn-10**). A similar shift (+210 mV) was observed when a second nitro group was added to **Mn-10** to yield **Mn-11**. The introduction of a nitro group to **Mn-13**, which possesses two *para*-alkyl substituents and an electron-withdrawing substituent (similarly to **Mn-10**) to give **Mn-14**, shifted the potential in the same extent as previously observed with **Mn-10** and **Mn-11**. A comparable shift (+170 mV) in the $Fe^{III}P/Fe^{II}P$ potential was observed following the *meso*-nitro substitution of Fe(III) β-octaethylporphyrin.[90] Such a high shift in potential of porphyrin redox or metal-centered redox properties is consistent with the strong electron-withdrawing power of the nitro group.[47,51,91,92] Although both **Mn-11** and **Mn-12** possess two nitro substituents, the difference in potentials observed (151 mV) is probably due to the electron-donating effect of the pentyl chains resulting in negative partial potentials as opposed to the electron-withdrawing effect of the CF_3 group. The morpholinomethyl substituent present in **Mn-15** results in a negative shift of the potential compared to **Mn-13**, due to its electron-donating effect.

From the data gathered, the following sequence can be established for the $Mn^{III}P/Mn^{II}P$ redox couple in response to the *meso* substituents: $CH_2NR < Ph < CF_3 \sim p\text{-}(Me_3N)C_6F_4 \sim C(O)Ph < NO_2 \sim$ oxo.

2.4. SOD activity

All compounds (**Mn-1**–**Mn-15**) were examined for SOD activity using the cytochrome *c* (cyt *c*) assay.[20] Although of appropriate potential ($E_{1/2}$ = +0.208 V), **Mn-12** had no detectable SOD activity. The SOD activity of **Mn-8**, which exhibits $E_{1/2}$ = +0.449 V versus NHE, could not be precisely determined due to its strong catalysis of cyt *c* reoxidation by H_2O_2. Yet, with catalase present, the log k_{cat} could be estimated to be equal to or lower than 4.60. None of the other compounds had any significant SOD-like activity (i.e. exhibiting log $k_{cat} \geqslant 4.60$) other than **Mn-1**, which exhibited a log k_{cat} = 5.20. The origin of the activity of **Mn-1** is not known, but may be associated with the polarity of the *meso*-carbonyl group. In this regard, a significant increase in SOD activity was observed upon replacement of an alkyl chain by an oxygenated side-chain within the $MnTE\text{-}2\text{-}PyP^{5+}$-type series (Chart 1).[24,25,45] The lack of activity of the remaining manganese porphyrin complexes, despite the presence of favorable $E_{1/2}$ values for some, may stem from the lack of positive charges close to the metal site. On the other hand, in a more lipophilic environment where the $E_{1/2}$ of $O_2/O_2^{\cdot-}$ is shifted negatively (e.g., from −160 mV (aqueous) to −600 mV vs NHE in DMF), some of the compounds may have electrochemical potentials sufficient to compensate for the lack of electrostatic attraction. Such may be the case with compounds **Mn-1**, **Mn-3**, **Mn-11**, and particularly **Mn-12**. Further study is required to address this issue.

Similar to the case with ubiquinone[1] and with naturally occurring polyphenols,[93] the compounds bearing *meso*-oxo substituents (**Mn-6** and **Mn-8**) upon reduction to the semiquinone radical could potentially produce superoxide. The production of superoxide may entail one-electron oxidation of the semiquinone radical by oxygen. Several compounds have already been used in in vivo studies whose anticancer ability has been explained through their ability to produce reactive species. Such compounds include texaphyrin, motexafin gadolinium, and parthenolide.[94–96] Thus, rather than SOD mimics, **Mn-6** and **Mn-8** may be considered for in vivo study of their anticancer effects due to their likelihood to produce superoxide and subsequently its progeny peroxynitrite.

3. Conclusion

The manganese porphyrins described herein represent new molecular designs that achieve redox control while maintaining low molecular weight and tailored lipophilicity. The limited molecular weight is a challenge given the intrinsic size of the porphyrin macrocycle. Control over these features is essential to meet the criteria for a catalytic antioxidant that crosses the blood–brain barrier and remains active in membranous structures. The new synthetic routes exploited herein illustrate the capabilities for gaining access to diverse molecular designs.

Although electrostatic facilitation for the reaction with $O_2^{\cdot-}$ cannot be provided when a lipophilic environment is targeted, compounds bearing benzoyl, nitro, and CF_3 functionalities (**Mn-1**, **Mn-3**, **Mn-11**, and in particular **Mn-12**) display metal-centered redox potentials positive enough that might allow them, along with tailored lipophilicity, to scavenge reactive species within cellular components (membranes) and organs (central nervous system) that are otherwise difficult to access. That would render them particularly promising for treating neurological disorders. Finally, compounds having *meso*-oxo substituents, **Mn-8** and **Mn-6**, may potentially be promising for killing cancer cells through production of reactive species.

4. Experimental

4.1. General synthesis procedures

^{1}H NMR (300 MHz) and ^{13}C NMR (75 MHz) spectra were recorded in $CDCl_3$ unless noted otherwise. Absorption spectra and fluorescence emission spectra were collected in CH_2Cl_2 at room temperature unless noted otherwise. Hydrophobic porphyrins were analyzed in neat form (without a matrix) by laser desorption mass spectrometry (LD–MS). Water-soluble porphyrins were analyzed by direct infusion of aqueous or methanolic solutions by atmospheric pressure electrospray mass spectrometry (ESI-MS). Elution was performed in a solvent mixture of water/acetonitrile (0.1% HCOOH) at a flow rate of 0.3 mL/min. Both in LD–MS and ESI-MS analyses, positive ions were detected unless noted otherwise. In general, the manganese porphyrins gave a parent molecule ion lacking the chloride counterion [i.e., $(M–Cl)^+$]. Infrared absorption spectra were recorded as KBr pellets. Melting points are uncorrected. Solvents were dried according to standard procedures. The progress of porphyrin-forming reactions was monitored by absorption spectroscopy. Porphyrin metalation reactions were monitored by TLC and fluorescence emission spectroscopy.

4.2. Chromatography

Preparative chromatography was performed using silica (40 μm average particle size) or alumina (80–200 mesh). Thin layer chromatography was performed on silica or alumina. Samples were visualized by ultraviolet light (254 and 365 nm). Analytical reversed-phase high pressure liquid chromatography (RP-HPLC) was carried out using an octadecylsilica column (5 μm, 125 × 4 mm) under the following elution conditions: flow rate = 1.0 mL/min; A = water (35%), B = methanol (0.1% TFA) (65%); detection at 254 and 450 nm.

4.3. Noncommercial compounds

The following compounds were prepared as described in the literature: Free base porphyrins **1**,[63] **2**,[63] **3**,[60] **4**,[60] and **19**;[70] dipyrromethanes **16**,[58,59] **17**,[59] and **18**;[60] and 1,9-diformyldipyrromethane **24**.[79] An alternative synthesis of the known porphyrin **5**[66,68,69] is reported here.

4.4. Manganese metalation procedures

4.4.1. Method A: Exemplified for *meso*-tetrabenzoyl porphinatomanganese(III)chloride (Mn-1). Following a literature procedure,[61] a solution of **1** (24 mg, 0.033 mmol) in $CHCl_3$/MeOH (2:1, 15 mL) was treated with $MnCl_2$ (66 mg, 0.53 mmol, 16 equiv) and 2,6-lutidine (six drops). The mixture was stirred at 50 °C for 36 h. Removal of solvent yielded a dark-green residue, which upon chromatography [silica, $CHCl_3$ → $CHCl_3$/MeOH (9:1)] afforded a greenish brown solid (18 mg, 69%): LD–MS obsd 778.9 $(M–Cl)^+$; FAB-MS obsd 779.1489, calcd 779.1491 ($C_{48}H_{28}MnN_4O_4$); λ_{abs} 370, 477, 577 nm.

4.4.2. Method B: Exemplified for 5,5,15,15-tetramethyl-10,20-diphenylporphodimethenatomanganese(III)chloride (Mn-5). Following a literature method,[62] a solution of **5** (80 mg, 0.15 mmol) was treated with $MnCl_2$ (0.25 g, 2.0 mmol, 13 equiv) in DMF (100 mL) and heated at reflux. After 2 h, an aliquot taken from the solution showed ~ 60% metalation according to the UV–vis spectrum. The reaction was allowed to proceed for another 2 h, during which time $MnCl_2$ (0.75 g, 6.0 mmol, 40 equiv) was added in portions. After cooling to room temperature, DMF was removed in vacuo, and the resulting crude solid was washed amply with H_2O and dried under vacuum. The solid was dissolved in CH_2Cl_2 (10 mL), to which silica gel (1–2 g) was added. The resulting slurry was concentrated to dryness. The resulting powder was poured on top of a silica column packed and eluted with CH_2Cl_2/MeOH (4:1). The product, an orange band, was collected and concentrated. The addition of hexanes yielded a precipitate (76 mg, 83%). Single crystals for X-ray diffraction were grown by slow vapor-phase diffusion of hexanes into a concentrated solution of **Mn-5** in $CHCl_3$: LD–MS obsd 573.2 $(M–Cl)^+$; FAB-MS obsd 573.1867, calcd 573.1851 ($C_{36}H_{30}MnN_4$); λ_{abs} 347, 428, 492 nm.

4.5. Synthesis of manganese porphyrins

4.5.1. 5-Benzoyl-10,15,20-tris(4-methylphenyl)porphinatomanganese(III)chloride (Mn-2). Metalation of **2** (21 mg, 0.030 mmol) following method A with chromatography [silica, $CHCl_3$ → $CHCl_3$/MeOH (98:2)] afforded a greenish brown solid (17 mg, 77%): LD–MS obsd 736.5 $(M–Cl)^+$; FAB-MS obsd 737.2133, calcd 737.2113 ($C_{48}H_{34}MnN_4O$); λ_{abs} 376, 401, 477, 581, 617 nm.

4.5.2. 5,15-Dibenzoyl-10,20-bis(trifluoromethyl)porphinatomanganese(III)chloride (Mn-3). Metalation of **3** (13 mg, 0.020 mmol) following method A with chromatography [silica, $CHCl_3$ → $CHCl_3$/MeOH (98:2)] afforded a greenish brown solid (12 mg, 85%): LD–MS obsd 706.7 $(M–Cl)^+$; FAB-MS obsd 707.0726, calcd 707.0714 ($C_{36}H_{18}F_6MnN_4O_2$); λ_{abs} 359, 427, 474, 573, 614 nm.

4.5.3. 5,15-Diphenyl-10,20-bis(trifluoromethyl)porphinatomanganese(III)chloride (Mn-4). Metalation of **4** (24 mg, 0.040 mmol) following method A with chroma-

tography [silica, $CHCl_3$/MeOH (19:1 → 9:1)] afforded a greenish brown solid (14 mg, 54%): LD–MS obsd 650.36 $(M–Cl)^+$; FAB-MS obsd 651.0833, calcd 651.0816 ($C_{34}H_{18}F_6MnN_4$); λ_{abs} 365, 475, 574, 617 nm.

4.5.4. 5,15-Dioxo-10,20-diphenylporphodimethenatomanganese(III)chloride (Mn-6). Following a procedure similar to method B, a solution of dioxoporphodimethene **6** (40 mg, 0.081 mmol) in DMF (60 mL) was treated with $MnCl_2$ (150 mg, 1.19 mmol, 14.7 equiv) at 100 °C. The mixture changed immediately from yellow to orange. The solution was heated at reflux and stirred. After 2 h, an aliquot taken from the reaction mixture showed ~ 85% metalation according to UV–vis absorption spectroscopy. Another portion of $MnCl_2$ (100 mg, 0.79 mmol, 9.8 equiv) was added, and the reaction was continued for 2 h. After cooling to room temperature, DMF was removed under vacuum. The resulting solid was dissolved in CH_2Cl_2 (100 mL) and a small amount of MeOH. The solution was washed with 0.01 M HCl (50 mL), dried (Na_2SO_4) and concentrated to afford an orange solid. Recrystallization (DMF/H_2O) afforded a green crystalline solid (36 mg, 77%): LD–MS obsd 545.3 $(M–Cl)^+$; FAB-MS obsd 546.0892, calcd 546.0888 ($C_{32}H_{19}MnN_4O_2$); IR: ν (CO), 1648 cm^{-1}; λ_{abs} (DMF) 347, 420, 454, 509, 544 nm.

4.5.5. 5,15-Di-*n*-pentylporphinatomanganese(III) chloride (Mn-9). Metalation of **9** (30.0 mg, 0.0665 mmol) following method A with chromatography [silica, CH_2Cl_2 → CH_2Cl_2/MeOH (19:1)] generated a green solid. The compound was dissolved in CH_2Cl_2 and washed twice with water. The organic layer was dried (Na_2SO_4) and filtered. The filtrate was concentrated to give a shiny green solid (32 mg, 95%): LD–MS obsd 503.4 $(M–Cl)^+$ and 538.5 (M^+, trace); FAB-MS obsd 503.2001, calcd 503.2007 ($C_{30}H_{32}MnN_4$) and 538.1696 (M = $C_{30}H_{32}ClMnN_4$); λ_{abs} 339, 367, 395, 473, 575, 607 nm.

4.5.6. 10-Nitro-5,15-di-*n*-pentylporphinatomanganese(III) chloride (Mn-10). Metalation of **10** (23 mg, 0.050 mmol) following method A over a period of 4 days followed by chromatography [silica, $CHCl_3$ → $CHCl_3$/MeOH (93:7)] gave a solid (26 mg, 100%): LD–MS obsd 547.8 $(M–Cl)^+$; FAB-MS obsd 548.1852, calcd 548.1858 ($C_{30}H_{31}MnN_5O_2$); λ_{abs} 477, 577, 618 nm.

4.5.7. 5,15-Dinitro-10,20-di-*n*-pentylporphinatomanganese(III) chloride (Mn-11). Following a procedure similar to method A, a solution of **11** (15.5 mg, 0.0287 mmol) in $CHCl_3$/MeOH (2:1, 13 mL) was treated with $MnCl_2$ (63.1 mg, 0.502 mmol, 17.5 equiv) and 2,6-lutidine (five drops). The mixture was stirred at reflux. The progress of the reaction was monitored by TLC. After 40 h, an additional 29 mg (0.23 mmol, 8 equiv) of $MnCl_2$ was added as some free base porphyrin was still detected upon TLC analysis. After a total of 50 h, the reaction had leveled off, whereupon the solvent was evaporated. The residue was dissolved in hexanes containing a small amount of CH_2Cl_2/MeOH (a previous attempt at the reaction showed signs of demetalation in the presence of CH_2Cl_2). The dissolution was facilitated by sonication. Chromatography [silica, hexanes → CH_2Cl_2/MeOH (9:1)] afforded a green solid (10.2 mg, 57%): LD–MS obsd 592.9 $(M–Cl)^+$; FAB-MS obsd 593.1726, calcd 593.1709 ($C_{30}H_{30}MnN_6O_4$); λ_{abs} (MeOH) 377, 426, 464, 564, 604 nm.

4.5.8. 5,15-Dinitro-10-(trifluoromethyl)porphinatomanganese(III)chloride (Mn-12). Metalation of **12** (9.4 mg, 0.020 mmol) following method A with chromatography [silica, $CHCl_3$ → $CHCl_3$/MeOH (9:1)] afforded a green solid (8.2 mg, 79%): LD–MS obsd 520.9 $(M–Cl)^+$; FAB-MS obsd 521.0023, calcd 521.0018 ($C_{21}H_9F_3MnN_6O_4$); λ_{abs} 353, 474, 569, 606 nm.

4.5.9. 5,15-Diisopropyl-10-(trifluoromethyl)porphinatomanganese(III)chloride (Mn-13). Metalation of **13** (15 mg, 0.033 mmol) following method A with chromatography [silica, $CHCl_3$ → $CHCl_3$/MeOH (9:1)] afforded a greenish brown solid (13 mg, 76%): LD–MS obsd 514.3 $(M–Cl)^+$; FAB-MS obsd 515.1266, calcd 515.1255 ($C_{27}H_{23}F_3MnN_4$); λ_{abs} 370, 474, 575 nm.

4.5.10. 5,15-Diisopropyl-10-nitro-20-(trifluoromethyl)porphinatomanganese(III)chloride (Mn-14). Metalation of **14** (11 mg, 0.022 mmol) following method A with chromatography [silica, $CHCl_3$ → $CHCl_3$/MeOH (9:1)] afforded a green solid (10 mg, 82%): LD–MS obsd 560.2 $(M–Cl)^+$; FAB-MS obsd 560.1129, calcd 560.1106 ($C_{27}H_{22}F_3MnN_5O_2$); λ_{abs} 362, 479, 581, 625 nm.

4.5.11. 5,15-Diisopropyl-10-(*N*-morpholinomethyl)-20-(trifluoromethyl)porphinatomanganese(III)chloride (Mn-15). Metalation of **15** (15.8 mg, 0.0281 mmol) following method A with chromatography [silica, $CHCl_3$/MeOH (9:1 → 6:4)] afforded a green solid (14 mg, 81%): LD–MS obsd 612.1 $(M–Cl)^+$; FAB-MS obsd 614.1963, calcd 614.1939 ($C_{32}H_{32}F_3MnN_5O$); λ_{abs} 374, 479, 584, 631 nm.

4.5.12. 5,15-Bis(2,3,5,6-tetrafluoro-4-dimethylaminophenyl)porphinatomanganese(III)chloride (Mn-21). Following method B, a solution of **21** (45 mg, 0.065 mmol) in DMF (20 mL) was treated with $MnCl_2$ (0.20 g, 1.6 mmol, 25 equiv) and the mixture was heated at reflux for 3 h. After cooling to room temperature, the DMF was removed in vacuo. The crude mixture was dissolved in CH_2Cl_2 (10 mL) and silica gel (1–2 g) was added. The resulting slurry was concentrated to dryness. The resulting red powder was placed on top of a silica column, which was eluted with CH_2Cl_2/MeOH (4:1). The product, a major orange band, was collected and concentrated to dryness. The residue was dissolved in CH_2Cl_2. The resulting solution was treated with hexanes to give a precipitate (28 mg, 55%): LD–MS obsd 745.4 $(M–Cl)^+$; FAB-MS obsd 745.1203, calcd 745.1159 ($C_{36}H_{22}F_8MnN_6$); λ_{abs} 322, 367, 390, 457, 547, 579, 760 nm.

4.5.13. 5,15-Bis(2,3,5,6-tetrafluoro-4-dimethylaminophenyl)-10,20-dioxoporphodimethenatomanganese(III)chloride (Mn-23). Following method B, a solution of **23** (10 mg, 0.014 mmol) in DMF (10 mL) was treated with $MnCl_2$ (100 mg, 0.80 mmol). The solution was heated at reflux for 3 h and then allowed to cool to room temper-

ature. The slow addition of H_2O afforded a precipitate, which was filtered, washed with H_2O and dried under vacuum, affording a green solid (9.8 mg, 86%): LD–MS obsd 775.3; FAB-MS obsd 776.0970, calcd 776.0979 [(M + H)$^+$, M = $C_{36}H_{20}F_8MnN_6O_2$]; λ_{abs} (3 mL CH_2Cl_2 + 150 μL DMF) 321, 464, 522, 560 nm.

4.6. Synthesis of porphyrin precursors

4.6.1. 1,9-Bis(*N*,*N*-dimethylaminomethyl)-5-trifluoromethyldipyrromethane (26). Following a standard procedure,[80] a solution of **18** (701 mg, 3.27 mmol) in CH_2Cl_2 (35 mL) at room temperature was treated with *N*,*N*-dimethylmethyleneiminium iodide (Eschenmoser's reagent) (1.304 g, 7.048 mmol, 2.15 equiv). After 1 h, CH_2Cl_2 (120 mL) and saturated aqueous $NaHCO_3$ (120 mL) were added to the reaction mixture. The organic phase was dried (Na_2SO_4) and then concentrated to afford a light brown solid (799 mg, 74%; ~95% pure): mp 80–85 °C (dec.); ^{1}H NMR δ 2.16 (s, 12H), 3.26–3.44 (m, 4H), 4.69 (m, 1H), 5.92–6.06 (m, 4H), 8.76 (br, 2H); ^{13}C NMR δ 43.7 (q, J = 29.6 Hz), 45.2, 56.7, 108.0, 108.8, 123.0, 125.4 (q, J = 278.4 Hz), 130.3; Anal. calcd for $C_{16}H_{23}F_3N_4$: C, 58.52; H, 7.06; N, 17.06; Found: C, 57.74; H, 6.90; N, 16.49.

4.6.2. 1,9-Diisobutyroyl-5-(trifluoromethyl)dipyrromethane (27). Following a standard procedure,[57] a solution of **18** (1.39 g, 6.50 mmol) in toluene (130 mL) was treated with a 1.0 M solution of EtMgBr in THF (32.5 mL, 32.5 mmol). The mixture was stirred for 15 min under argon. A solution of isobutyroyl chloride (2.00 mL, 19.5 mmol) in toluene (20 mL) was slowly added. The reaction mixture was stirred for 20 min. The reaction was quenched by addition of saturated aqueous NH_4Cl. Ethyl acetate was added and the organic phase was separated. The organic layer was washed (water then brine) and dried (Na_2SO_4). The solvent was removed to afford a dark residue, which was chromatographed [silica, CH_2Cl_2/hexanes (2:1)] to afford a pale brown solid (972 mg, 42%): mp 193–194 °C; ^{1}H NMR δ 1.23 (d, J = 6.6 Hz, 12H), 3.31 (sept, J = 6.6 Hz, 2H), 5.30 (m, 1H), 6.38 (m, 2H), 6.95 (m, 2H), 10.32 (br, 2H); ^{13}C NMR δ 19.85, 35.86, 43.35 (q, J = 31.2 Hz), 110.71, 117.41, 124.81 (q, J = 279.1 Hz), 130.73, 131.37, 196.00; Anal. Calcd for $C_{18}H_{21}F_3N_2O_2$: C, 61.01; H, 5.97; N, 7.91. Found: C, 60.58; H, 6.01; N, 7.80; FAB-MS obsd 355.1646, calcd 355.1646 [(M + H)$^+$, M = $C_{18}H_{21}F_3N_2O_2$].

4.7. Synthesis of A-, trans-A_2-, and trans-AB_2C-porphyrins

4.7.1. 5,15-Di-*n*-pentylporphyrin (9). A sample of Montmorillonite K10 (1 g) was activated (100 °C, < 30 mm Hg) for 2 h in a 250 mL flask and then cooled to room temperature under argon. To the flask were added CH_2Cl_2 (95 mL), hexanal (60 μL, 0.49 mmol), and a solution of dipyrromethane **17** (73 mg, 0.50 mmol) in CH_2Cl_2 (5 mL). The resulting mixture was stirred at room temperature for 1 h, then solid *p*-chloranil (190 mg, 0.77 mmol) was added. The reaction mixture was heated at reflux for 1 h. Solid materials were removed by filtration through a Celite pad and washed with $CHCl_3$. The filtrate was concentrated, and the crude product was purified by chromatography [silica, CH_2Cl_2/hexanes (1:1) → CH_2Cl_2] to afford a purple solid (62 mg, 56%): ^{1}H NMR δ −2.94 (br, 2 H), 0.96 (t, J = 7.4 Hz, 6H), 1.48–1.60 (m, 4H), 1.73–1.83 (m, 4H), 2.48–2.59 (m, 4H), 4.98 (t, J = 8.1 Hz, 4H), 9.38 (d, J = 4.2 Hz, 4H), 9.55 (d, J = 4.8 Hz, 4H), 10.14 (s, 2H); LD–MS obsd 450.2; FAB-MS obsd 451.2852 calcd 451.2862 [(M + H)$^+$, M = $C_{30}H_{34}N_4$]; λ_{abs} 404, 503, 535, 578, 633 nm.

4.7.2. 5,15-Diisopropyl-10-(trifluoromethyl)porphyrin (13). Following a general procedure,[57] $NaBH_4$ (2.27 g, 60.0 mmol) was added in portions over 5 min to a solution of **27** (1.06 g, 3.00 mmol) in THF/MeOH (10:1, 165 mL) under argon. The reaction mixture was stirred at room temperature for 40 min, whereupon TLC examination showed a single product. The reaction mixture was poured into a mixture of saturated aqueous NH_4Cl (150 mL) and CH_2Cl_2 (200 mL). The organic phase was separated, washed (water) and dried (Na_2SO_4). The solvent was removed to give **27-diol**. The latter was placed in a 2 L round-bottom flask containing **17** (0.438 g, 3.00 mmol) in CH_3CN (1.2 L). This mixture was stirred for 5 min to achieve complete dissolution. TFA (2.80 mL, 36 mmol) was added in a slow steady stream. The condensation was monitored by UV–vis spectroscopy. After 4 min of condensation, DDQ (2.04 g, 9.00 mmol) was added. The mixture was stirred at room temperature for 1 h. Triethylamine (5.00 mL, 36 mmol) was added, and the mixture was filtered through a pad of alumina and eluted with CH_2Cl_2 until the eluate was no longer dark. The resulting porphyrin-containing solution was concentrated to yield a dark solid. The dark solid was dissolved in CH_2Cl_2 (30 mL) and passed through a pad of silica [CH_2Cl_2/hexanes (2:1)]. The fractions containing the desired porphyrin (fast-eluting) were combined and concentrated to afford a purple solid (216 mg, 16%): ^{1}H NMR δ −2.35 (br, 2H), 2.39 (d, J = 7.2 Hz, 12H), 5.51 (m, 2H), 9.29 (d, J = 5.1 Hz, 2H), 9.56–9.65 (m, 6H), 10.04 (s, 1H); LD–MS obsd 462.54; FAB-MS obsd 462.2007, calcd 462.2031 ($C_{27}H_{25}F_3N_4$); λ_{abs} 409, 510, 544, 585, 640 nm.

4.7.3. 5,15-Bis(pentafluorophenyl)porphyrin (20). A solution of dipyrromethane **17** (438 mg, 3.00 mmol) and pentafluorobenzaldehyde (588 mg, 3.00 mmol) in $CHCl_3$ (300 mL) was degassed with a continuous stream of Ar for 10 min before being treated with $BF_3{\cdot}OEt_2$ (120 μL, 0.97 mmol). The reaction vessel was shielded from ambient light and stirred under Ar for 3 h. DDQ (2.04 g, 8.99 mmol) was added to the reaction mixture, and stirring was continued for 1 h. After removal of the solvent, the crude mixture was dissolved in CH_2Cl_2 (10 mL). Silica gel (1–2 g) was added. The resulting slurry was concentrated to dryness and chromatographed [silica, CH_2Cl_2/hexanes (4:1)] to afford a purple solid (120 mg, 12%): ^{1}H NMR δ −3.26 (br, 2H), 9.01 (d, J = 4.4 Hz, 4H), 9.49 (d, J = 4.4 Hz, 4H), 10.40 (s, 2H); LD–MS obsd 642.4; FAB-MS obsd 642.0947, calcd 642.0902 ($C_{32}H_{12}F_{10}N_4$); λ_{abs} 400, 498, 530, 572, 626 nm.

4.7.4. 5-Trifluoromethylporphyrin (25). Following a general procedure,[57] reduction of **24** (540 mg, 2.00 mmol) followed by condensation with **17** (292 mg, 2.00 mmol) for 2 h, oxidation with DDQ (1.36 mg, 6.00 mmol) and standard workup and chromatography on silica (CH_2C1_2) furnished a purple solid (57 mg, 8%): ^{1}H NMR δ −3.64 (br, 2H), 9.35–9.55 (m, 6H), 9.79 (m, 2H), 10.23 (s, 1H), 10.28 (s, 2H); LD–MS obsd 377.54; FAB-MS obsd 379.1177, calcd 379.1171 [(M + H)$^+$, M = $C_{21}H_{13}F_3N_4$]; λ_{abs} 395, 495, 528, 570, 619 nm.

4.7.5. 5-Trifluoromethylporphinatozinc(II) (Zn-25). Following a standard procedure,[80] a solution of **26** (588 mg, 1.79 mmol) and dipyrromethane **17** (266 mg, 1.82 mmol) in EtOH (184 mL) at room temperature was treated with $Zn(OAc)_2$ (3.31 g, 18.0 mmol, 9.9 equiv). The mixture was heated to reflux. After 2 h, the reaction mixture was allowed to cool to room temperature. A sample of DDQ (1.24 g, 5.46 mmol) was added, and the mixture was stirred for 15 min. Triethylamine (1.27 mL, 11.8 mmol) was added, and the reaction mixture was concentrated to dryness. Column chromatography (silica, hexanes → CH_2Cl_2) afforded a bright pink solid (83.6 mg, 11%): ^{1}H NMR (THF-d_8) δ 9.5–9.6 (m, 6H), 9.83–9.88 (m, 2H), 10.38 (s, 2H), 10.41 (s, 1H); LD–MS obsd 440.0; FAB-MS obsd 440.0215, calcd 440.0227 ($C_{21}H_{11}F_3N_4Zn$); λ_{abs} 397, 531, 568 nm.

4.8. Synthesis of porphodimethenes and dioxoporphodimethenes

4.8.1. 5,5,15,15-Tetramethyl-10,20-diphenylporphodimethene (5). A solution of **16** (2.32 g, 13.3 mmol) and benzaldehyde (1.35 mL, 13.3 mmol) in CH_2Cl_2 (250 mL) was degassed with a continuous stream of argon for 10 min before the addition of TFA (103 μL, 1.34 mmol). After stirring for 2 h at room temperature, DDQ (3.44 g, 15.1 mmol) was added to the reaction mixture, and stirring was continued for 1 h. The solvent was removed in vacuo. The resulting residue was chromatographed (silica, CH_2Cl_2), affording a yellow solution which was concentrated to ∼10 mL. The slow addition of methanol afforded a red crystalline solid (330 mg, 10%): ^{1}H NMR δ 1.95 (s, 12H), 6.24 (d, J = 4.2 Hz, 4H), 6.32 (d, J = 4.2 Hz, 4H), 7.34–7.47 (m, 10H), 14.17 (br, 2H); LD–MS obsd 520.5; FAB-MS obsd 520.2648, calcd 520.2627 ($C_{36}H_{32}N_4$); Anal Calcd for $C_{36}H_{32}N_4$: C, 83.04; H. 6.19; N, 10.76; Found: C, 82.93; H, 6.24; N, 10.72; λ_{abs} 321, 423, 488 nm. The characterization data of the sample prepared by this procedure are identical to those reported in the literature.[68]

4.8.2. 5,15-Dioxo-10,20-diphenylporphodimethene (6). Following a literature procedure,[71] a solution of **19** (0.100 g, 0.220 mmol) and TFA (6.25 mL, 81.1 mmol) in CH_2Cl_2 (32 mL) was treated dropwise over 5 min with a solution of thallium(III) trifluoroacetate (TTFA, 2.2 g, 4.0 mmol) in TFA (6 mL). The mixture turned from blue to green and then slowly to yellow-green. After 20 min, the solution was poured into 250 mL of H_2O and washed with another portion of H_2O (250 mL), yielding an orange-red organic layer. The organic phase was collected, dried (Na_2SO_4) and concentrated, affording a brown thallium(III) complex. Demetalation was carried out immediately by dissolving the crude material in TFA (5 mL) and stirring for 1 h. The resulting yellow solution was poured into water, and CH_2Cl_2 (200 mL) was added. The organic layer was washed with several portions of H_2O, dried (Na_2SO_4), and concentrated. Chromatography [silica, hexanes/CH_2Cl_2 (1:2 → 1:5)] afforded an uncharacterized fraction (pale green) followed by the desired product (yellow solution). The solvent was removed, and the resulting black solid was recrystallized from hot toluene (46 mg, 43%): ^{1}H NMR δ 6.20–6.80 (br, 4H), 7.17 (d, J = 4.4 Hz, 4H), 7.40–7.60 (m, 10H), 14.01 (br, 2H); LD–MS obsd 492.3; FAB-MS obsd 492.1599, calcd 492.1586; Anal Calcd for $C_{36}H_{20}N_4O_2$: C, 78.04; H, 4.09; N, 11.38; Found: C, 78.15; H, 4.13; N, 11.35; IR: ν (CO), 1618 cm^{-1}; λ_{abs} (EtOH/CH_2Cl_2) 343, 408, 473, 499 nm.

4.8.3. 5,15-Dioxo-10,20-diphenylporphodimethenatozinc(II) (Zn-6). A solution of **6** (40 mg, 0.081 mmol) in CH_2Cl_2 (50 mL) was treated with $Zn(OAc)_2{\cdot}2\,H_2O$ (150 mg, 0.68 mmol) in MeOH (5 mL). The reaction mixture was heated at reflux for 1 h. The solvent was removed in vacuo. The solid was dissolved in a minimum amount of CH_2Cl_2/MeOH (98:2) and chromatographed [silica, CH_2Cl_2/MeOH (98:2)]. Concentration of the major fraction afforded a purple solid (42 mg, 93%): ^{1}H NMR (pyridine-d_5) δ 6.65 (d, J = 4.4 Hz, 4H), 7.42–7.58 (m, 14H); LD–MS obsd 554.3; FAB-MS obsd 554.0757, calcd 554.0721 ($C_{32}H_{18}N_4O_2Zn$); IR: ν (CO), 1506 cm^{-1}; λ_{abs} (EtOH/CH_2C1_2) 352, 410, 450, 510, 547 nm.

4.8.4. 5,15-Dioxo-10,20-bis(pentafluorophenyl)porphodimethene (22). Following a similar procedure as for the preparation of **6**, a solution of **20** (162 mg, 0.250 mmol) in CH_2Cl_2 (35 mL) containing TFA (10 mL) was treated with a solution of TTFA (1.1 g, 2.0 mmol) in TFA (10 mL). The reaction was continued for 40 min then the resulting purple solution was washed with H_2O (2 × 250 mL). The organic phase was dried (Na_2SO_4) and concentrated. The demetalation was carried out immediately by dissolving the solid in TFA (35 mL) with stirring overnight. After washing with H_2O (3 × 250 mL), drying (Na_2SO_4) and concentrating the organic layer, the resulting brown solution was chromatographed (silica, CH_2Cl_2). The yellow solution was collected and concentrated to dryness, affording a black crystalline solid (98 mg, 58%): ^{1}H NMR (CD_2Cl_2) δ 6.51 (br, 4H), 7.25 (d, J = 4.2 Hz, 4H), 13.75 (s, 2H); IR: ν (CO), 1583 cm^{-1}; LD–MS obsd 672.3; FAB-MS obsd 673.0751, calcd 673.0722 [(M + H)$^+$, M = $C_{32}H_{10}F_{10}N_4O_2$]; λ_{abs} 312, 411, 478, 502 nm.

4.9. Synthesis of nitroporphyrins

4.9.1. 10-Nitro-5,15-di-*n*-pentylporphinatozinc(II) (Zn-10). An ice-cooled mixture of fuming nitric acid (4.8 mL) and glacial acetic acid (4.8 mL) was added to a solid sample of **9** (50 mg, 0.11 mmol). The resulting

green mixture was stirred at 0 °C for 20 min and an additional 5 min after removing the ice bath. The solution was poured into ice water (100 mL) and extracted with $CHCl_3$. The organic layer was washed with aqueous $NaHCO_3$ and brine, dried over Na_2SO_4, and concentrated. The resulting purple solid, an inseparable mixture of mononitroporphyrin and dinitroporphyrin products, was used directly in the ensuing metalation reaction. The mixture of nitroporphyrins **10** and **11** (54 mg) was dissolved in CH_2Cl_2 (95 mL) and treated with a solution of $Zn(OAc)_2{\cdot}2H_2O$ (2.4 g, 11 mmol) in MeOH (10 mL). The resulting green reaction mixture was stirred overnight and then poured into saturated aqueous $NaHCO_3$. The organic layer was separated and dried (Na_2SO_4). Chromatography (silica, toluene) gave **Zn-10** as the first band (26 mg, 43%) and **Zn-11** as the second band (4 mg, 7%). **Zn-10**: ^{1}H NMR (DMSO-d_6) δ 0.89 (t, J = 7.4 Hz, 6H), 1.39–1.58 (m, 4H), 1.63–1.80 (m, 4H), 2.32–2.48 (m, 4H), 4.98 (m, 4H), 9.26 (d, J = 4.6 Hz, 2H), 9.47 (d, J = 4.6 Hz, 2H), 9.65 (d, J = 4.6 Hz, 2H), 9.76 (d, J = 4.6 Hz, 2H), 10.26 (s, 1H); LD–MS obsd 556.4; FAB-MS obsd 557.1760, calcd 557.1769 ($C_{30}H_{31}N_5O_2Zn$); λ_{abs} 413, 547, 591 nm.

4.9.2. 10-Nitro-5,15-di-*n*-pentylporphyrin (10). Demetalation of **Zn-10** (26 mg, 0.047 mmol) with TFA generated the corresponding free base porphyrin (23 mg, 100%): ^{1}H NMR δ –2.93 (br, 2H), 0.95 (t, J = 7.2 Hz, 6H), 1.46–1.59 (m, 4H), 1.70–1.80 (m, 4H), 2.42–2.53 (m, 4H), 4.88 (t, J = 8.1 Hz, 4H), 9.29–9.31 (m, 4H), 9.42–9.44 (m, 2H), 9.50–9.52 (m, 2H), 10.09 (s, 1H); LD–MS obsd 495.3; FAB-MS obsd 496.2692, calcd 496.2713 ($C_{30}H_{33}N_5O_2$); λ_{abs} 410, 513, 552, 585, 644 nm.

4.9.3. 5,15-Dinitro-10,20-di-*n*-pentylporphinatozinc(II) (Zn-11). Zinc(II) nitrate hexahydrate (53 mg, 0.18 mmol) was added to a solution of porphyrin **9** (20 mg, 0.044 mmol) in acetic anhydride (6 mL) and the mixture was stirred at room temperature for 20 min. The mixture was then poured into water and extracted with CH_2Cl_3. The organic solution was washed with saturated aqueous $NaHCO_3$ and brine, dried over Na_2SO_4, and concentrated. The residue was dissolved in a small amount of $CHCl_3$ and chromatographed (silica, $CHCl_3$). The green band was the desired zinc porphyrin (13 mg, 49%): ^{1}H NMR (DMSO-d_6) δ 0.90 (t, J = 7.2 Hz, 6H), 1.40–1.53 (m, 4H), 1.66–1.77 (m, 4H), 2.31–2.44 (m, 4H), 4.97 (t, J = 7.5 Hz, 4H), 9.31 (d, J = 4.8 Hz, 4H), 9.78 (d, J = 4.8 Hz, 4H); LD–MS obsd 601.4; FAB-MS obsd 602.1631, calcd 602.1620 ($C_{30}H_{30}N_6O_4Zn$); λ_{abs} (DMSO/CH_2Cl_2) 428, 555, 600, 627 nm.

4.9.4. 5,15-Dinitro-10,20-di-*n*-pentylporphyrin (11). Demetalation of porphyrin **Zn-11** (33 mg, 0.055 mmol) with TFA yielded the corresponding free base porphyrin (24 mg, 80%): ^{1}H NMR δ –3.03 (br, 2H), 0.95 (t, J = 7.5 Hz, 6H), 1.46–1.60 (m, 4H), 1.68–1.80 (m, 4H), 2.39–2.52 (m, 4H), 4.87 (*t*, J = 8.0 Hz, 4H), 9.27 (d, J = 5.1 Hz, 4H), 9.49 (d, J = 5.1 Hz, 4H); LD–MS obsd 540.1; FAB-MS obsd 541.2578, calcd 541.2563 ($C_{30}H_{32}N_6O_4$); λ_{abs} 416, 516, 558, 596, 655 nm.

4.9.5. 5,15-Dinitro-10-(trifluoromethyl)porphinatozinc(II) and 5,20-Dinitro-10-(trifluoromethyl)porphinatozinc(II) (Zn-12). A suspension of **Zn-25** (43.8 mg, 0.0992 mmol) in acetic anhydride (4.05 mL) was sonicated to help dissolve the porphyrin complex, treated with $Zn(NO_3)_2{\cdot}6H_2O$ (72.9 mg , 0.245 mmol, 2.47 equiv), and stirred at room temperature for 40 min. The mixture was then poured into water and extracted with CH_2Cl_2. The organic solution was washed with saturated aqueous $NaHCO_3$ and brine, dried (Na_2SO_4), and concentrated to afford a green purple residue. The latter was dried under vacuum to remove any traces of acetic anhydride. The crude solid was dissolved in a small amount of CH_2Cl_2 (with sonication) and chromatographed [silica, $CH_2Cl_2 \rightarrow CH_2Cl_2$/MeOH (99:1)] to yield a purple solid (22 mg). The column was stripped with CH_2Cl_2/MeOH, and the solvent was evaporated. The resulting solid residue was submitted to a second column under similar conditions to obtain additional purple solid (combined mass = 30.5 mg, 58%): ^{1}H NMR (THF-d_8) δ 9.36–9.56 (m, 9H), 9.78 (m, 2H), 9.88 (m, 4H), 10.41 (s, 2H), 10.49 (s, 1H); LD–MS obsd 530.0; FAB-MS obsd 529.9931, calcd 529.9929; λ_{abs} 412, 548, 586 nm.

An identical method was used for the synthesis of **Zn-12** from **25**: $Zn(NO_3){\cdot}6H_2O$ (35.6 mg, 0.120 mmol) was added to a solution of porphyrin **25** (18.9 mg, 0.0500 mmol) in acetic anhydride (2 mL), and the mixture was stirred at room temperature for 40 min. Aqueous-organic work-up followed by chromatography afforded **Zn-12** (16.3 mg, 61%).

4.9.6. 5,15-Dinitro-10-(trifluoromethyl)porphyrin (12). A sample of **Zn-12** (22 mg, 0.041 mmol) was stirred overnight in TFA (4 mL) at room temperature. The reaction was monitored by treating a small aliquot from the reaction mixture with $NaHCO_3$ followed by UV–vis spectroscopy. Upon completion, saturated aqueous $NaHCO_3$ was added slowly to neutralize the acid in the reaction mixture. The organic phase was extracted with CH_2Cl_2, washed (water), and dried (Na_2SO_4). The organic layer was concentrated to yield a purple residue, which was chromatographed (silica, CH_2Cl_2) to afford a purple-brown solid (24.5 mg, 96%): ^{1}H NMR (DMF-d_7) δ 9.50–10.0 (m, 24H), 10.83 (s, 2H), 10.88 (s, 1H), inner protons were not visible due to poor solubility; ^{1}H NMR (pyridine-d_5) δ –4.31 (br, 6H) (barely seen), 9.40–9.70 (m, 18H), 9.75–9.85 (m, 6H), 10.36 (s, 2H), 10.37 (s, 1H); LD–MS obsd 468.1, calcd 468.1 ($C_{21}H_{11}F_3N_6O_4$); λ_{abs} (1 drop of compound dissolved in DMF, then diluted in CH_2Cl_2) 408, 507, 544, 585, 640 nm.

4.9.7. 5,15-Diisopropyl-10-nitro-20-(trifluoromethyl)porphinatozinc(II) (Zn-14). $Zn(NO_3){\cdot}6H_2O$ (30 mg, 0.10 mmol) was added to a solution of **13** (46 mg, 0.10 mmol) in $CHC1_3$ (2 mL) and acetic anhydride (0.5 mL). The resulting mixture was stirred at room temperature for 3 min, poured into water, and extracted with $CHCl_3$. The organic solution was washed with saturated aqueous $NaHCO_3$ and brine, dried over Na_2SO_4, and concentrated. The resulting residue was dissolved in a small amount of $CHCl_3$ and chromatographed (silica,

CH_2Cl_2) to give first a purple band, starting material **13**, followed by a green band corresponding to the mono-nitro porphyrin. The green band was collected and concentrated to afford a green-purple solid (18 mg, 32%): ^{1}H NMR δ 2.42 (d, J = 7.2 Hz, 12H), 5.66 (m, 2H), 9.36 (d, J = 5.4 Hz, 2H), 9.80 (m, 6H); LD–MS obsd 568.2; FAB-MS obsd 569.1044, calcd 569.1017 ($C_{27}H_{22}F_3N_5O_2Zn$); λ_{abs} 416, 553, 592 nm.

4.9.8. 5,15-Diisopropyl-10-nitro-20-(trifluoromethyl)porphyrin (14). A solution of **Zn-14** (17.0 mg, 0.030 mmol) in TFA (2 mL) was stirred at room temperature for 1 h. The reaction was monitored by treating a small aliquot from the reaction mixture with $NaHCO_3$ followed by UV–vis spectroscopy. Upon completion, saturated aqueous $NaHCO_3$ was added slowly to neutralize the acid in the reaction mixture. The organic phase was extracted with CH_2Cl_2, washed (water), and dried (Na_2SO_4). The organic layer was concentrated to yield a purple residue, which upon chromatography (silica, CH_2Cl_2) afforded a purple-brown solid (13 mg, 87%): ^{1}H NMR δ −2.34 (br, 2H), 2.37 (d, J = 7.5 Hz, 12H), 5.45 (m, 2H), 9.25 (d, J = 5.1 Hz, 2H), 9.57–9.65 (m, 6H); LD–MS obsd 507.3; FAB-MS obsd 508.1972, calcd 508.1960 [$(M + H)^+$, M = $C_{27}H_{24}F_3N_5O_2$]; λ_{abs} 413, 516, 557, 597, 657 nm.

4.10. Amination of pentafluorophenyl-substituted compounds

4.10.1. 5,15-Bis(2,3,5,6-tetrafluoro-4-dimethylaminophenyl)porphyrin (21). A solution of **20** (50 mg, 0.080 mmol) and $(CH_3)_2NH{\cdot}HCl$ (2.0 g, 25 mmol) in DMF (50 mL) was stirred at 120 °C under argon for 24 h. The solvent was removed in vacuo. The resulting solid was dissolved in CH_2Cl_2 (100 mL) and washed with H_2O (50 mL). The organic phase was dried (Na_2SO_4), concentrated, and chromatographed [silica, hexanes/CH_2Cl_2 (1:3)]. Trace amounts of unreacted starting material and a mono-4-dimethylaminophenyl-substituted porphyrin were collected prior to the desired porphyrin as an orange-red solution. Removal of the solvent afforded a purple solid (42 mg, 78%): ^{1}H NMR δ −3.20 (br, 2H), 3.30 (t, J = 2.1 Hz, 12H), 9.09 (d, J = 4.5 Hz, 4H), 9.44 (d, J = 4.5 Hz, 4H), 10.33 (s, 2H); LD–MS obsd 692.5; FAB-MS obsd 692.1960, calcd 692.1935 ($C_{36}H_{24}F_8N_6$); λ_{abs} 405, 500, 534, 573, 628 nm.

4.10.2. 5,15-Bis(2,3,5,6-tetrafluoro-4-dimethylaminophenyl)-10,20-dioxoporphodimethene (23). A solution of **22** (75 mg, 0.11 mmol) and $(CH_3)_2NH{\cdot}HCl$ (3.00 g, 36.8 mmol) in DMF (75 mL) was stirred at 120 °C under argon for 24 h. After cooling to room temperature, the DMF was removed in vacuo. The resulting solid was dissolved in CH_2Cl_2 and washed with water (twice). The organic phase was dried (Na_2SO_4), concentrated, and chromatographed [silica, hexanes/CH_2Cl_2 (1:1 → 1:2.5)]. Traces of a mono-4-dimethylaminophenylporphyrin were collected prior to the desired product as a yellow-orange solution. Removal of the solvent afforded a black crystalline solid (45 mg, 57%). A single crystal for X-ray diffraction was obtained by slow vapor-phase diffusion of methanol into a concentrated solution of **23** in CH_2Cl_2: ^{1}H NMR δ 3.08 (s, 12H), 6.4–6.7 (br, 4H), 7.22 (d, J = 4.6 Hz, 4H), 13.87 (br, 2H); LD–MS obsd 721.5; FAB-MS obsd 722.1622, calcd 722.1676 ($C_{36}H_{22}F_8N_6O_2$); IR: ν (CO), 1588 cm^{-1}; λ_{abs} 306, 412, 479, 503 nm.

4.10.3. 5,15-Bis(2,3,5,6-tetrafluoro-4-dimethylaminophenyl)-10,20-dioxoporphodimethenatozinc(II) (Zn-23). A solution of **23** (22.5 mg, 0.0311 mmol) in $CHCl_3$ (2.5 mL) and MeOH (1 mL) was treated with $Zn(OAc)_2$ (56 mg, 0.31 mmol, 9.9 equiv). The resulting mixture was stirred at room temperature open to the air. After 75 min, some starting material was still visible on TLC, therefore additional $Zn(OAc)_2$ (38.5 mg, 0.210 mmol, 6.75 equiv) was added along with 0.5 mL of $CHCl_3$ and 0.5 mL MeOH. After a total of 165 min, the reaction was stopped. During the course of the reaction, the initial dark yellowish solution turned deep red. CH_2Cl_2 was added to the reaction mixture, and the resulting mixture was washed with dilute aqueous $NaHCO_3$ (once) and with water (twice). The organic layer was dried (Na_2SO_4) and filtered. The filtrate was concentrated and dried in vacuo, generating a crystalline dark pink solid (20.7 mg, 85%): ^{1}H NMR (CD_2Cl_2/CD_3OD, 9:1) δ 3.05 (tr, J = 2.1 Hz, 12H), 6.54 (d, J = 4.2 Hz, 4H), 7.07 (d, J = 4.5 Hz, 4H); LD–MS obsd 784.2; FAB-MS obsd 784.0819, calcd 784.0811 ($C_{36}H_{20}F_8N_6O_2Zn$); λ_{abs} 325, 461, 522, 561 nm.

4.11. Quaternization of dimethylaminoporphyrins

4.11.1. [5,15-Bis(2,3,5,6-tetrafluoro-4-trimethylammoniumylphenyl) porphinatomanganese(III)] trifluoromethanesulfonate (Mn-7). Following a literature procedure,[75] **Mn-21** (24 mg, 0.031 mmol) and freshly distilled methyl trifluoromethanesulfonate (150 μL, 1.33 mmol, 43 equiv) were stirred in trimethylphosphate (15 mL) under argon at 60 °C. After 12 h, MeOH (2 mL) was added to quench unreacted methyl trifluoromethanesulfonate. The reaction mixture was slowly added to 100 mL of rapidly stirred diethyl ether. The precipitate obtained was filtered, washed with copious amounts of diethyl ether to remove trimethylphosphate, and dried under vacuum, affording a brown solid (20 mg, 52% yield; 45% yield on the basis of the elemental analysis): Anal. Calcd for **Mn-7**·$(CH_3O)_3PO{\cdot}H_2O$ ($C_{44}H_{39}F_{17}MnN_6O_{14}PS_3$): C, 38.27; H, 2.85; N, 6.09; F, 23.39; S, 6.97; Found: C, 37.98; H, 2.81; N, 6.11; F, 23.61; S, 7.03; ESI-MS obsd 462.1 $[M–(CF_3SO_3)_2]^{2+}$ and 258.5 $[M–(CF_3SO_3)_3]^{3+}$; FAB-MS obsd 1073.0682 $[M–(CF_3SO_3)]^+$, calcd 1073.0669 ($C_{40}H_{28}F_{14}MnN_6O_6S_2$); λ_{abs} (H_2O) 364, 453, 543, 576, 762 nm; RP-HPLC t_R = 11.35 min.

4.11.2. [5,15-Dioxo-10,20-bis(2,3,5,6-tetrafluoro-4-trimethylammoniumylphenyl)porphodimethenatomanganese(III)] trifluoromethanesulfonate (Mn-8). Following a similar procedure as described for the preparation of **Mn-7**, samples of **Mn-23** (9.8 mg, 0.012 mmol) and methyl trifluoromethanesulfonate (56 μL, 0.5 mmol, 42 equiv) were stirred in trimethylphosphate (5 mL) at 60 °C under argon. After 12 h, MeOH (1 mL) was added to quench unreacted methyl trifluoromethanesulfonate. The reaction mixture was slowly added to 50 mL of rap-

idly stirred diethyl ether. The precipitate obtained was filtered, washed with copious amounts of diethyl ether to remove trimethylphosphate, and dried under vacuum, affording a green solid (10 mg, 67% yield; 55% yield on the basis of the elemental analysis): Anal. Calcd for **Mn-8**·2$(CH_3O)_3PO$ ($C_{47}H_{44}F_{17}MnN_6O_{18}P_2S_3$): C, 36.83; H, 2.89; N, 5.48; F, 21.07; S, 6.28. Found: C, 36.51; H, 2.83; N, 5.53; F, 21.53; S, 6.35; ESI-MS obsd 477.0 $[M–(CF_3\ SO_3)_2]^{2+}$ 402.5 $[M–(CF_3\ SO_3)_3]^{2+}$, 268.4 $[M–(CF_3\ SO_3)_3]^{3+}$, calcd 954.1 ($C_{39}H_{26}F_{11}MnN_6O_5S$), 805.1 ($C_{38}H_{26}F_8MnN_6O_2$); λ_{abs} (H_2O) 341, 391, 442, 463, 573, 606, 724, 795 nm. Attempts to collect a high-resolution FAB-MS spectrum were unsuccessful.

4.11.3. Zinc(II)-[5,15-dioxo-10,20-bis(2,3,5,6-tetrafluoro-4-trimethylammoniumphenyl)porphodimethene]trifluoromethanesulfonate (Zn-8). Following a literature procedure,[75] **Zn-23** (9.7 mg, 0.012 mmol) and methyl trifluoromethanesulfonate (180 μL, 1.59 mmol, 129 equiv) were stirred in trimethylphosphate (5 mL) under argon at 60 °C. The reaction was followed by ESI-MS spectrometry. After 19 h, no peaks corresponding to the starting material (m/z = 784) or the mono-alkylated compound (m/z = 799) were noticeable; therefore, 1 mL of MeOH was added to quench any unreacted methyl trifluoromethanesulfonate. After cooling the reaction mixture to room temperature, the solution was slowly added to ~50 mL of vigorously stirred diethyl ether. The dark green precipitate generated was filtered, washed with copious amounts of diethyl ether to remove any trace of trimethylphosphate and then dissolved in MeOH. Removal of the solvent afforded a dark greenish purple solid (10 mg, 73%): ^{1}H NMR (CD_3OD) δ 4.00 (s, 18H), 6.66 (d, J = 4.2 Hz, 4H), 7.11 (d, J = 4.5 Hz, 4H); ESI-MS obsd 407.0 $[M–(CF_3SO_3)_2]^{2+}$, calcd 1112.0 ($C_{40}H_{26}F_{14}N_6O_8S_2Zn$), 814.1 ($C_{38}H_{26}F_8N_6O_2Zn$); λ_{abs} (MeOH) 324, 410, 456, 520, 558 nm. Attempts to collect a high-resolution FAB-MS spectrum were unsuccessful.

4.12. Synthesis of morpholinylporphyrins

4.12.1. 5,15-Diisopropyl-10-(*N*-morpholinomethyl)-20-(trifluoromethyl)porphyrin (15). A solution of **28** (78 mg, 0.16 mmol) in CH_2Cl_2/MeOH (3:1, 8 mL) was treated with morpholine (0.084 mL, 0.96 mmol) and $NaBH_3CN$ (8.0 mg, 0.12 mmol). The mixture was stirred at reflux for 48 h. During the course of the reaction, the reaction mixture turned from green to purple. The reaction mixture was cooled to room temperature, and water was added. The mixture was extracted with CH_2Cl_2. The organic layer was dried (Na_2SO_4) and concentrated to afford a purple residue. ^{1}H NMR analysis of the crude reaction mixture indicated the presence of the reductively aminated product and a reduced product in the ratio of 2.5:1. The mixture was then chromatographed (alumina, CH_2Cl_2). The first purple band was collected and concentrated to afford a purple solid (52 mg, 58%): ^{1}H NMR δ −1.93 (br, 2H), 2.35 (d, J = 7.2 Hz, 12 H), 2.77 (t, J = 4.5 Hz, 4H), 3.64 (t, J = 4.5 Hz, 4H), 5.38 (m, 2H), 5.56 (s, 2H), 9.47–9.60 (m, 8H); LD–MS obsd 559.3; FAB-MS obsd 561.2739; calcd 561.6407 ($C_{32}H_{34}F_3N_5O$); λ_{abs} 417, 518, 594, 651 nm. The second purple band was eluted and the solvent was removed to afford hydroxymethyl-porphyrin **29** as a purple solid (20 mg, 25%): ^{1}H NMR δ −2.04 (br, 2H), 2.35 (d, J = 7.5 Hz, 12 H), 2.67 (br, 1H), 5.40 (m, 2H), 6.77 (d, J = 3.6 Hz, 2H), 9.50–9.60 (m, 8H); LD–MS obsd 490.8; FAB-MS obsd 492.2131, calcd 492.2137 ($C_{28}H_{27}F_3N_4O$); λ_{abs} (toluene) 418, 517, 552, 595, 652 nm; λ_{abs} (CH_2Cl_2 + three drops MeOH) 414, 516, 551, 592, 650 nm.

4.12.2. 5,15-Diisopropyl-10-(*N*-morpholinomethyl)-20-(trifluoromethyl)porphinatozinc(II) (Zn-15). A solution of **15** (47 mg, 0.083 mmol) in $CHCl_3$ (6 mL) was treated with $Zn(OAc)_2·2H_2O$ (37 mg, 0.17 mmol) in MeOH (0.5 mL). The resulting mixture was stirred overnight at room temperature. The reaction mixture was poured into saturated aqueous $NaHCO_3$. The organic layer was separated, washed (water), dried (Na_2SO_4) and concentrated to afford a purple residue. The residue was chromatographed [alumina, CH_2Cl_2/ethyl acetate (2:1)] to afford a purple solid (46 mg, 89%): ^{1}H NMR δ 1.55 (s, 4H), 1.72 (s, 4H), 2.35 (d, J = 7.2 Hz, 12H), 5.10 (s, 2H), 5.55 (m, 2H), 9.30 (d, J = 5.1 Hz, 2H), 9.53 (d, J = 4.2 Hz, 2H), 9.63–9.73 (m, 4H); LD–MS obsd 620.9; FAB-MS obsd 623.1831, calcd 623.1850 ($C_{32}H_{32}F_3N_5OZn$); λ_{abs} 418, 553, 587 nm.

4.12.3. 5-Formyl-10,20-diisopropyl-15-(trifluoromethyl)porphinatozinc(II) (Zn-28). A solution of **28** (49 mg, 0.10 mmol) in $CHCl_3$ (6 mL) was treated with $Zn(OAc)_2·2H_2O$ (44 mg, 0.20 mmol) in methanol (0.5 mL), and the mixture was stirred at room temperature for 4 h. The reaction mixture was poured into saturated aqueous $NaHCO_3$. The organic layer was separated, washed (water), dried (Na_2SO_4), concentrated, and chromatographed (silica, CH_2Cl_2) to afford a green-purple solid (51 mg, 93%): ^{1}H NMR δ 2.39 (d, J = 7.2 Hz, 12H), 5.58 (m, 2H), 9.67–9.87 (m, 8H); 12.01 (s, 1H); LD–MS obsd 552.56, calcd 552.11 ($C_{28}H_{23}F_3N_4OZn$); λ_{abs} (toluene) 428, 568, 613 nm.

4.12.4. 5,15-Diisopropyl-10-(trifluoromethyl)porphinatocopper(II) (Cu-13). A solution of **13** (102 mg, 0.220 mmol) in $CHCl_3$/MeOH (1:1, 20 mL) was treated with $Cu(OAc)_2·H_2O$ (1.10 g, 5.50 mmol). The mixture was stirred at room temperature for 2 h. Removal of the solvent yielded a red residue, which upon chromatography [alumina, CH_2Cl_2/hexanes (2:1)] afforded a red solid (109 mg, 95%): LD–MS obsd 522.58; FAB-MS obsd 523.1188, calcd 523.1271 ($C_{27}H_{23}F_3CuN_4$); λ_{abs} 409, 541, 574 nm.

4.12.5. 5-Formyl-10,20-diisopropyl-15-(trifluoromethyl)porphinatocopper(II) (Cu-28). A solution of **Cu-13** (0.105 g, 0.200 mmol) in CH_2Cl_2 (10 mL) was treated with a Vilsmeier solution [prepared freshly from DMF (0.100 mL, 1.29 mmol) and $POCl_3$ (0.100 mL, 1.10 mmol) at 0 °C]. The resulting mixture was heated at reflux. After 2 h, TLC examination displayed a large amount of starting material; thus, additional Vilsmeier reagent [DMF (0.100 mL, 1.29 mmol) and $POCl_3$ (0.100 mL, 1.10 mmol) at 0 °C] was added. The mixture was heated at reflux for 6 h, at which time additional

Vilsmeier reagent [DMF (0.100 mL, 1.29 mmol) and $POCl_3$ (0.100 mL, 1.10 mmol)] was added, the reaction remaining incomplete. The mixture was then heated overnight at reflux. During the course of the reaction, the reaction mixture turned from red to green. After cooling to room temperature, saturated aqueous $NaHCO_3$ (10 mL) was slowly added, and the mixture was stirred at room temperature for 2 h. The organic phase was extracted with CH_2Cl_2, washed (water), and dried (Na_2SO_4). The solvent was removed to give a green residue, which upon chromatography (silica, CH_2Cl_2) afforded a purple-green solid (96 mg, 87%): LD–MS obsd 549.6; FAB-MS obsd 551.1112, calcd 551.1220 ($C_{28}H_{23}CuF_3N_4O$); λ_{abs} 423, 569, 613 nm.

4.12.6. 5-Formyl-10,20-diisopropyl-15-(trifluoromethyl)porphyrin (28). A solution of **Cu-28** (0.10 g, 0.18 mmol) in TFA (10 mL) was treated with concentrated H_2SO_4 (5 mL). The mixture was stirred overnight at room temperature. The reaction was monitored by treating a small aliquot from the reaction mixture with $NaHCO_3$ followed by UV–vis spectroscopy. Upon completion, saturated aqueous $NaHCO_3$ was added slowly to neutralize the acid in the reaction mixture. The organic phase was extracted with CH_2Cl_2, washed (water), and dried (Na_2SO_4). The organic layer was concentrated to yield a purple residue, which upon chromatography (silica, CH_2Cl_2) afforded a purple solid (84 mg, 96%): ^{1}H NMR δ −1.83 (br, 2H), 2.33 (d, J = 6.6 Hz, 12H), 5.35 (m, 2H), 9.51–9.62 (m, 6H), 9.93 (d, J = 5.1 Hz, 2H), 12.31 (s, 1H); LD–MS obsd 490.2; FAB-MS obsd 490.1967, calcd 490.1980 ($C_{28}H_{25}F_3N_4O$); λ_{abs} (toluene) 424, 530, 573, 615, 675 nm.

4.13. Electrochemistry

Measurements were performed on a CH Instruments Model 600 Voltammetric Analyzer.[12] The apparatus consisted of a three-electrode system composed of a glassy carbon button working electrode (3-mm diameter) from Bioanalytical Systems, a Ag/AgCl reference electrode, and a Pt auxiliary electrode. The experiments were performed in a small volume cell (0.5–3 mL) using argon-purged MeOH/H_2O (9:1) solutions containing 0.05 M tris buffer, pH 7.8, 0.1 M NaCl, and 0.5 mM metalloporphyrin. The analysis of **Mn-1** was carried out in DMF/H_2O (9:1). Either MnTE-2-PyP^{5+} or its methyl analogue, MnTM-2-PyP^{5+}, was used as a reference. The redox couples of the references were measured in both solvent systems employed for the study of the manganese porphyrin complexes, with or without the manganese porphyrin of interest present in the solution. In the former case, we made sure that the redox couples of both the reference and the studied porphyrin were independent. In either case, the differences between these values are within 10 mV. The scan rates were 0.01–0.5 V/s, typically 0.1 V/s, except with **Mn-11**, where the scan rate was 0.02 V/s.

The required correction for the potential going from a reference of MeOH/H_2O versus Ag/AgCl to a 100% aqueous system versus NHE is on average 96 ± 10 mV. This value corresponds to the difference in potential for MnTE-2PyP^{5+} between the two experimental conditions. In the case of **Mn-1**, a correction value of 28 mV was added in going from DMF/H_2O (vs Ag/AgCl) to the value obtained in an aqueous system (vs NHE).

Voltammograms of ferrocenemethanol and MnTM-2-PyP^{5+} were also obtained in an aqueous solution containing 0.05 M tris buffer, pH 7.8, 0.1 M NaCl. The purpose of these experiments was to determine if an identical solvent effect was observed with both compounds when the medium was changed from MeOH/water to water. Since the shifts in potential were identical, the potentials were standardized against either MnTE-2-PyP^{5+} or its methyl analogue, MnTM-2-PyP^{5+}.[97]

4.14. Catalysis of $O_2^{\cdot-}$ disproportionation

The catalytic rate constants for the $O_2^{\cdot-}$ disproportionation were determined by cytochrome *c* assay as previously described.[24,27,89,98] Stock solutions of manganese porphyrins were prepared in methanol (except **Mn-1**, which was dissolved in DMF). Stock solutions were then diluted into the assay mixture. The control, uninhibited cytochrome *c* reduction, was performed with the same concentration of methanol or DMF. Xanthine/xanthine oxidase (40 μM xanthine, ~ 2 nM xanthine oxidase) was the source of $O_2^{\cdot-}$, and ferricytochrome *c* was used as the indicating scavenger of $O_2^{\cdot-}$. The reduction of cyt *c* was followed at 550 nm. Assays were conducted at 25 ± 1 °C in 0.05 M phosphate buffer, pH 7.8, 0.1 mM EDTA in the presence or absence of 15 μg/mL catalase. Rate constants for the reaction of metalloporphyrins with $O_2^{\cdot-}$ were based upon the competition with 10 μM cyt *c*; $k_{cyt\ c}$ = 2.6×10^5 M^{-1} s^{-1} as described elsewhere.[27] The $O_2^{\cdot-}$ was produced at 1.2 μM/min. Any possible interference of manganese porphyrins with production of $O_2^{\cdot-}$ was examined following urate formation at 295 nm in the absence of cyt *c*. Also the possible reoxidation of cyt *c* with manganese porphyrins and H_2O_2 or cyt *c* reduction enhancement that could affect the assay outcome was studied. The former was assessed by reduction of cyt *c* with sodium dithionite in 0.05 M phosphate buffer, pH 7.8, whereupon the manganese porphyrin was added. The value of k_{cat} was calculated based on the concentration that caused 50% inhibition of the cyt *c* reduction.[89]

Acknowledgments

This work was supported by grants from the NIH (IR21-ESO/3682, U19 AI67798-01) to I.B.H. and J.S.R., the NIH/NCI Duke Comprehensive Cancer Center Core Grant (5-P30-CA14236-29) to I.S., and the NIH (GM36238) to J.S.L. Mass spectra were obtained at the Mass Spectrometry Laboratory for Biotechnology at North Carolina State University. Partial funding for the facility was obtained from the North Carolina Biotechnology Center and the NSF. We thank Prof. Irwin Fridovich for stimulating discussions.

Supplementary data

Supplementary data associated with this article can be found, in the online version, at doi:10.1016/j.bmc.2007.07.015.

References and notes

1. (a) Halliwell, B.; Gutteridge, J. M. C. In *Free Radicals in Biology and Medicine*, third ed.; Oxford University Press, 1999; (b) Gutteridge, J. M. C. *Free Rad. Res. Comm* **1993**, *19*, 141–158; (c) Halliwell, B. *Biochem. J.* **2007**, *401*, 1–11; (d) Halliwell, B. *Plant Physiol.* **2006**, *141*, 312–322.
2. Fridovich, I. *Ann. Rev. Biochem.* **1995**, *64*, 97–112.
3. Dworakowski, R.; Anilkumar, N.; Zhang, M.; Shah, A. M. *Biochem. Soc. Trans.* **2006**, *34*, 960–964.
4. Infanger, D. W.; Sharma, R. V.; Davisson, R. L. *Antioxid. Redox Signal.* **2006**, *8*, 1583–1596.
5. (a) Cuzzocrea, S. *Pharmacol. Res.* **2005**, *52*, 72–82; (b) Muravchick, S.; Levy, R. J. *Anesthesiology* **2006**, *105*, 819–836; (c) Jones, D. P. *Antioxid. Redox Signal.* **2006**, *8*, 1865–1879; (d) World, C. J.; Yamawaki, H.; Berk, B. C. *J. Mol. Med.* **2006**, *84*, 997–1003; (e) Sasaki, Y. *J. Gastroenterol.* **2006**, *41*, 1135–1148; (f) Szeto, H. H. *AAPS J.* **2006**, *8*, E521–E531; (g) Browne, S. E.; Beal, M. F. *Antioxid. Redox Signal.* **2006**, *8*, 2061–2073; (h) Lin, M. T.; Beal, M. F. *Nature* **2006**, *443*, 787–795; (i) Valko, M.; Leibfritz, D.; Moncol, J.; Cronin, M. T. D.; Mazur, M.; Telser, J. *Int. J. Biochem. Cell Biol.* **2007**, *39*, 44–84; (j) Madamanchi, N. R.; Runge, M. S. *Circ. Res.* **2007**, *100*, 460–473; (k) Trushina, E.; McMurray, C. T. *Neurosci.* **2007**, *145*, 1233–1248; (l) Whitton, P. S. *Br. J. Pharmacol.* **2007**, *150*, 963–976.
6. (a) Denicola, A.; Radi, R. *Toxicol.* **2005**, *208*, 273–288; (b) Lancaster, J. R., Jr. *Chem. Res. Toxicol.* **2006**, *19*, 1160–1174; (c) Pacher, P.; Beckman, J. S.; Liaudet, L. *Physiol. Rev.* **2007**, *87*, 315–424; (d) Demicheli, V.; Quijano, C.; Alvarez, B.; Radi, R. *Free Radic. Biol. Med.* **2007**, *42*, 1359–1368.
7. Wood, P. M. *Biochem. J.* **1988**, *253*, 287–289.
8. Vance, C. K.; Miller, A.-F. *J. Am. Chem. Soc.* **1998**, *120*, 461–467.
9. Ellerby, L. M.; Cabelli, D. E.; Graden, J. A.; Valentine, J. S. *J. Am. Chem. Soc.* **1996**, *118*, 6556–6561.
10. Michel, E.; Nauser, T.; Sutter, B.; Bounds, P. L.; Koppenol, W. H. *Arch. Biochem. Biophys.* **2005**, *439*, 234–240.
11. Goldstein, S.; Fridovich, I.; Czapski, G. *Free Radical Biol. Med.* **2006**, *41*, 937–941.
12. Spasojevic, I.; Batinic-Haberle, I.; Reboucas, J. S.; Idemori, Y. M.; Fridovich, I. *J. Biol. Chem* **2003**, *278*, 6831–6837.
13. Pardridge, W. M. In *Introduction to the Blood–Brain Barrier*; Pardridge, W. M., Ed.; Cambridge University Press: Cambride, UK, 1998; pp 1–8.
14. Imlay, J. A. *Mol. Microbiol.* **2006**, *59*, 1073–1082.
15. Pasternack, R. F.; Halliwell, B. *J. Am. Chem. Soc.* **1979**, *101*, 1026–1031.
16. Pasternack, R. F.; Skowronek, W. R., Jr. *J. Inorg. Biochem.* **1979**, *11*, 261–267.
17. Batinic-Haberle, I.; Benov, L.; Spasojevic, I.; Fridovich, I. *J. Biol. Chem.* **1998**, *273*, 24521–24528.
18. Lee, J.; Hunt, J. A.; Groves, J. T. *J. Am. Chem. Soc.* **1998**, *120*, 6053–6061.
19. Ferrer-Sueta, G.; Batinic-Haberle, I.; Spasojevic, I.; Fridovich, I.; Radi, R. *Chem. Res. Toxicol.* **1999**, *12*, 442–449.
20. Batinic-Haberle, I.; Spasojevic, I.; Hambright, P.; Benov, L.; Crumbliss, A. L.; Fridovich, I. T. *Inorg. Chem.* **1999**, *38*, 4011–4022.
21. Batinic-Haberle, I. *Methods Enzymol.* **2002**, *349*, 223–233.
22. Batinic-Haberle, I.; Spasojevic, I.; Stevens, R. D.; Hambright, P.; Fridovich, I. *J. Chem. Soc., Dalton Trans.* **2002**, 2689–2696.
23. Ferrer-Sueta, G.; Vitturi, D.; Batinic-Haberle, I.; Fridovich, I.; Goldstein, S.; Czapski, G.; Radi, R. *J. Biol. Chem.* **2003**, *278*, 27432–27438.
24. Batinic-Haberle, I.; Spasojevic, I.; Stevens, R. D.; Hambright, P.; Neta, P.; Okado-Matsumoto, A.; Fridovich, I. *Dalton Trans.* **2004**, 1696–1702.
25. Batinic-Haberle, I.; Spasojevic, I.; Stevens, R. D.; Bondurant, B.; Okado-Matsumoto, A.; Fridovich, I.; Vujaskovic, Z.; Dewhirst, M. W. *Dalton Trans.* **2006**, 617–624.
26. Ferrer-Sueta, G.; Hannibal, L.; Batinic-Haberle, I.; Radi, R. *Free Radic. Biol. Med.* **2006**, *41*, 503–512.
27. Saba, H.; Batinic-Haberle, I.; Munusamy, S.; Mitchell, T.; Lichti, C.; Megyesi, J.; MacMillan-Crow, L. A. *Free Radic. Biol. Med.* **2007**, *42*, 1571–1578.
28. Spasojevic, I.; Chen, Y.; Noel, T. J.; Yu, Y.; Cole, M. P.; Zhang, L.; Zhao, Y.; Clair, D. K. St.; Batinic-Haberle, I. *Free Radical Biol. Med.* **2007**, *42*, 1193–1200.
29. Lee, J.; Hunt, J. A.; Groves, J. T. *J. Am. Chem. Soc* **1998**, *120*, 7493–7501.
30. Shimanovich, R.; Groves, J. T. *Arch. Biochem. Biophys.* **2001**, *387*, 307–317.
31. Obrosova, I. G.; Mabley, J. G.; Zsengeller, Z.; Charniauskaya, T.; Abatan, O. I.; Groves, J. T.; Szabo, C. *FASEB J.* **2005**, *19*, 401–403.
32. Soule, B. P.; Hyodo, F.; Matsumoto, K.-I.; Simone, N. L.; Cook, J. A.; Krishna, M. C.; Mitchell, J. B. *Free Radical Biol. Med.* **2007**, *42*, 1632–1650.
33. Riley, D. P. *Adv. Supramol. Chem.* **2000**, *6*, 217–244.
34. Salvemini, D.; Riley, D. P.; Cuzzocrea, S. *Nat. Rev. Drug Disc.* **2002**, *1*, 367–374.
35. Olcott, A. P.; Tocco, G.; Tian, J.; Zekzer, D.; Fukuto, J.; Ignarro, L.; Kaufman, D. L. *Diabetes* **2004**, *53*, 2574–2580.
36. Morten, K. J.; Ackrell, B. A. C.; Melov, S. *J. Biol. Chem.* **2006**, *281*, 3354–3359.
37. James, A. M.; Cocheme, H. M.; Smith, R. A. J.; Murphy, M. P. *J. Biol. Chem.* **2005**, *280*, 21295–21312.
38. Dhanasekaran, A.; Kotamraju, S.; Karunakaran, C.; Kalivendi, S. V.; Thomas, S.; Joseph, J.; Kalyanaraman, B. *Free Radical Biol. Med.* **2005**, *39*, 567–583.
39. Asayama, S.; Kawamura, E.; Nagaoka, S.; Kawakami, H. *Mol. Pharm.* **2006**, *3*, 468–470.
40. Warner, D. S.; Sheng, H.; Batinic-Haberle, I. *J. Exp. Biol.* **2004**, *207*, 3221–3231.
41. Tse, H. M.; Milton, M. J.; Piganelli, J. D. *Free Radical Biol. Med.* **2004**, *36*, 233–247.
42. Moeller, B. J.; Cao, Y.; Li, C. Y.; Dewhirst, M. W. *Cancer Cell* **2004**, *5*, 429–441.
43. Zhao, Y.; Chaiswing, L.; Oberley, T. D.; Batinic-Haberle, I.; Clair, W. St.; Epstein, C. J.; St. Clair, D. *Cancer Res.* **2005**, *65*, 1401–1405.
44. Spasojevic, I.; Zhang, L.; Chen, Y.; Noel, T. J.; Cole, M. P.; Zhao Y.; Reboucas, J. S.; St. Clair, D. K.; Batinic-Haberle, I. *Int. Conf. Rad. Res.* San Francisco **2007**.
45. Okado-Matsumoto, A.; Batinic-Haberle, I.; Fridovich, I. *Free Radical Biol. Med.* **2004**, *37*, 401–410.
46. Giraudeau, A.; Callot, H. J.; Jordan, J.; Ezhar, I.; Gross, M. *J. Am. Chem. Soc.* **1979**, *101*, 3857–3862.
47. Worthington, P.; Hambright, P.; Williams, R. F. X.; Feldman, M. R.; Smith, K. M.; Langry, K. C. *Inorg. Nucl. Chem. Lett.* **1980**, *16*, 441–447.

48. Worthington, P.; Hambright, P.; Williams, R. F. X.; Reid, J.; Burnham, C.; Shamim, A.; Turay, J.; Bell, D. M.; Kirkland, R.; Little, R. G.; Datta-Gupta, N.; Eisner, U. *J. Inorg. Biochem.* **1980**, *12*, 281–291.
49. Gong, L.-C.; Dolphin, D. *Can. J. Chem.* **1985**, *63*, 401–405.
50. Rao, S.; Krishnan, V. *J. Mol. Struct.* **1994**, *327*, 279–285.
51. Ghosh, A. *J. Am. Chem. Soc.* **1995**, *117*, 4691–4699.
52. Rivkin, A.; Biswas, K.; Chou, T.-C.; Danishefsky, S. J. *Org. Lett.* **2002**, *4*, 4081–4084.
53. Wilson, R. M.; Danishefsky, S. J. *J. Org. Chem.* **2006**, *71*, 8329–8351.
54. Ojima, I.; Inoue, T.; Chakravarty, S. *J. Fluorine Chem.* **1999**, *97*, 3–10.
55. Gryshuk, A.; Chen, Y.; Goswami, L. N.; Pandey, S.; Missert, J. R.; Ohulchanskyy, T.; Potter, W.; Prasad, P. N.; Oseroff, A.; Pandey, R. K. *J. Med. Chem.* **2007**, *50*, 1754–1767.
56. Littler, B. J.; Ciringh, Y.; Lindsey, J. S. *J. Org. Chem.* **1999**, *64*, 2864–2872.
57. Rao, P. D.; Dhanalekshmi, S.; Littler, B. J.; Lindsey, J. S. *J. Org. Chem.* **2000**, *65*, 7323–7344.
58. Brown, W. H.; French, W. N. *Can. J. Chem.* **1958**, *36*, 371–377.
59. Littler, B. J.; Miller, M. A.; Hung, C.-H.; Wagner, R. W.; O'Shea, D. F.; Boyle, P. D.; Lindsey, J. S. *J. Org. Chem.* **1999**, *64*, 1391–1396.
60. Nishino, N.; Wagner, R. W.; Lindsey, J. S. *J. Org. Chem.* **1996**, *61*, 7534–7544.
61. Borovkov, V. V.; Lintuluoto, J. M.; Inoue, Y. *Synlett* **1999**, 61–62.
62. Adler, A. D.; Longo, F. R.; Kampas, F.; Kim, J. *J. Inorg. Nucl. Chem.* **1970**, *32*, 2443–2445.
63. Lindsey, J. S.; Prathapan, S.; Johnson, T. E.; Wagner, R. W. *Tetrahedron* **1994**, *50*, 8941–8968.
64. Benech, J.-M.; Bonomo, L.; Solari, E.; Scopelliti, R.; Floriani, C. *Angew. Chem. Int. Ed.* **1999**, *38*, 1957–1959.
65. Kral, V.; Sessler, J. L.; Zimmerman, R. S.; Seidel, D.; Lynch, V.; Andrioletti, B. *Angew. Chem. Int. Ed.* **2000**, *39*, 1055–1058.
66. Bucher, C.; Seidel, D.; Lynch, V.; Kral, V.; Sessler, J. L. *Org. Lett.* **2000**, *2*, 3103–3106.
67. Bischoff, I.; Feng, X.; Senge, M. O. *Tetrahedron* **2001**, *57*, 5573–5583.
68. Hong, S.-J.; Ka, J.-W.; Won, D.-H.; Lee, C.-H. *Bull. Korean Chem. Soc.* **2003**, *24*, 661–663.
69. Sharada, D. S.; Muresan, A. Z.; Muthukumaran, K.; Lindsey, J. S. *J. Org. Chem.* **2005**, *70*, 3500–3510.
70. Manka, J. S.; Lawrence, D. S. *Tetrahedron Lett.* **1989**, *30*, 6989–6992.
71. Barnett, G. H.; Hudson, M. F.; McCombie, S. W.; Smith, K. M. *J. Chem. Soc., Perkin Trans. I* **1973**, 691–696.
72. Fuhrhop, J.-H.; Baumgartner, E.; Bauer, H. *J. Am. Chem. Soc.* **1981**, *103*, 5854–5861.
73. Lindsey, J. S.; Wagner, R. W. *J. Org. Chem.* **1989**, *54*, 828–836.
74. Kadish, K. M.; Han, B. C.; Franzen, M. M.; Araullo-McAdams, C. *J. Am. Chem. Soc.* **1990**, *112*, 8364–8368.
75. La, T.; Richards, R.; Miskelly, G. M. *Inorg. Chem.* **1994**, *33*, 3159–3163.
76. Wiehe, A.; Shaker, Y. M.; Brandt, J. C.; Mebs, S.; Senge, M. O. *Tetrahedron* **2005**, *61*, 5535–5564.
77. Bonnett, R.; Stephenson, G. F. *J. Org. Chem.* **1965**, *30*, 2791–2798.
78. Laszlo, P.; Pennetreau, P. *J. Org. Chem.* **1987**, *52*, 2407–2410.
79. Wickramasinghe, A.; Jaquinod, L.; Nurco, D. J.; Smith, K. M. *Tetrahedron* **2001**, *57*, 4261–4269.
80. Fan, D.; Taniguchi, M.; Yao, Z.; Dhanalekshmi, S.; Lindsey, J. S. *Tetrahedron* **2005**, *61*, 10291–10302.
81. Fischer, H.; Gottschlich, R.; Seelig, A. *J. Membrane Biol.* **1998**, *165*, 201–211.
82. Xiong, Y.; Peterson, P. L.; Muizellaar, J. P.; Lee, C. P. *J. Neurotrauma* **1997**, *14*, 907–917.
83. Brenner, E.; Baldwin, R. M.; Tamagnan, G. *Org. Lett.* **2005**, *7*, 937–939.
84. Brockmann, V. H., Jr.; Bliesener, K.-M.; Inhoffen, H. H. *Liebigs Ann. Chem* **1968**, *718*, 148–161.
85. Ley, S. V.; Bolli, M. H.; Hinzen, B.; Gervois, A.-G.; Hall, B. J. *J. Chem. Soc. Perkin Trans. 1* **1998**, 2239–2242.
86. Hoffmann, P.; Robert, A.; Meunier, B. *Bull. Soc. Chim. Fr.* **1992**, *129*, 85–97.
87. Tsuchiya, S.; Seno, M. *Chem. Lett.* **1989**, 263–266.
88. Spasojevic, I.; Batinic-Haberle, I. *Inorg. Chim. Acta* **2001**, *317*, 230–242.
89. Spasojevic, I.; Batinic-Haberle, I.; Stevens, R. D.; Hambright, P.; Thorpe, A. N.; Grodkowski, J.; Neta, P.; Fridovich, I. *Inorg. Chem.* **2001**, *40*, 726–739.
90. Gong, L.; Yang, X. *Acta Chim. Sinica* **1985**, *43*, 302–305.
91. Sen, A.; Krishnan, V. *J. Chem. Soc., Faraday Trans.* **1997**, *93*, 4281–4288.
92. Ozette, K.; Battioni, P.; Leduc, P.; Bartoli, J.-F.; Mansuy, D. *Inorg. Chim. Acta* **1998**, *272*, 4–6.
93. Halliwell, B. *Cardiovasc. Res.* **2007**, *73*, 341–347.
94. Guzman, M. L.; Rossi, R. M.; Karnischky, L.; Li, X.; Peterson, D. R.; Howard, D. S.; Jordan, C. T. *Blood* **2005**, *105*, 4163–4169.
95. Hashemy, S. I.; Ungerstedt, J. S.; Avval, F. Z.; Holmgren, A. *J. Biol. Chem.* **2006**, *281*, 10691–10697.
96. Rosenberg, A.; Knox, S. *Int. J. Rad. Oncol. Biol. Phys.* **2006**, *64*, 343–354.
97. Aslan, M.; Ryan, T. M.; Adler, B.; Townes, T. M.; Parks, D. A.; Thompson, J. A.; Tousson, A.; Gladwin, M. T.; Patel, R. P.; Tarpey, M. M.; Batinic-Haberle, I.; White, C. R.; Freeman, B. A. *Proc. Natl. Acad. Sci. U.S.A.* **2001**, *98*, 15215–15220.
98. McCord, J. M.; Fridovich, I. *J. Biol. Chem.* **1969**, *244*, 6049–6055.